Table 1. Cont.

The Huh7.25.CD81 cells, seeded at 3.10^6 cells in 10-cm plates, were transfected after 24 hrs with 25 nM of siRNA Control or siRNA PKR using Fugene HD. 24 hrs post transfection, they were either mock-infected or infected for 2 hrs at 37°C with JFH1 (moi = 0.2) (three independent plates/sample). The medium was then removed and cells were incubated with complete DMEM for 12 hrs at 37°C. The cells were washed twice with TBS containing phosphatase and protease inhibitors, harvested by scraping, the cell pellets were centrifuged, the supernatants were removed and the pellets were frozen and stored at −80°C before being processed for micro-array.The list shows genes that were affected no more than twice by the depletion of PKR in the control cells (0.5< siPKR mock/siCt <1.6). The dependence of each of these genes in regards with PKR for their induction by HCV is expressed as log2 (ratio (siPKR HCV/siCt Mock)−(siCt HCV/siCt Mock) (indicated by log2*) with a cut-off of ≈2.0 fold.

doi:10.1371/journal.ppat.1002289.t001

pinpoint ISG15 as among the predictor genes of non-response to IFN therapy [14,15,16].

At present, we do not know at which level ISGylation regulates IFN induction in response to HCV infection. An HCV-mediated increase of ISG15 would favour preferential binding of ISG15 over that of ubiquitin to the E2 enzyme UbcH8 and hence enhance the spatio-temporal availability of UbcH8-ISG15 for HERC5 over that of UbcH8-ubiquitin for TRIM25. It may also lead to inhibition of TRIM25, through autoISGylation [21,34], which would decrease its ability to ubiquitinate RIG-I. We showed that overexpression of HERC5 together with Ubc1L, UbcH8 and ISG15 was increasing the ability of ISG15 to inhibit IFN induction by HCV (**Figure 2B**). All three enzymes Ubc1L, UbcH8 and HERC5 belong to the family of genes induced by IFN and it has been reported that ISGylation is optimum in a context of IFN treatment [18,35]. Therefore, it is tempting to speculate that elevated levels of ISG15 in some HCV-infected patients would bring the most favourable context for the virus when those patients are under IFN therapy. This would be in accord with the clinical data showing that HCV-induced high expression of ISG act as a negative predictive marker for response to IFN therapy.

It is doubtful that viruses with high IFN-inducing efficiency, such as Sendai virus may control RIG-I through ISG15 and PKR. However, viruses that avoid inducing IFN may have use of the PKR pathway. A good example might be that of Hepatitis B Virus (HBV) [36,37,38]. PKR expression was previously reported to be elevated in HCC liver from chronically HBV infected patients [39] and a relationship between PKR and IFN induction during HBV infection would be important to evaluate.

At present, we have established that HCV RNA interacts with PKR as soon as 2 hours post-infection. This interaction occurs prior the interaction of HCV RNA with RIG-I, which suggests that PKR may rapidly detect structures containing the incoming HCV RNA genome. Indeed, PKR has been reported to bind the dsRNA domains III and IV of HCV IRES [40] in addition to its ability to also bind 5′ triphosphorylated ss or dsRNA structures [41]. Whether PKR behaves as a pathogen recognition receptor for HCV RNA, like RIG-I, remains to be clarified. It is however clear that, in contrast to RIG-I, PKR acts here in favour of the pathogen rather than in favour of the host defense. We have established that the HCV RNA/PKR interaction depends on the first DRBD present at the N terminus of PKR and is independent on its kinase activity. The ability of PKR to serve as adapter in signaling pathways is not a total surprise since it has been previously shown to activate NF-κB through interaction of its C terminus with members of the TRAF family, such as TRAF5 and TRAF6 [42]. PKR contains also TRAF interacting motif in its N terminus [42] and an association between TRAF3 and PKR has been reported upon cotransfection in 293T cells [43]. Intriguingly, PKR was previously reported to participate in the induction of IFNβ, in association with MAVS, through activation of NF-κB or ATF-2 but not or partially IRF3; however these studies were not performed in the absence of RIG-I [44,45,46]. The mode of interaction between PKR, TRAF3 and MAVS, independently of RIG-I, and how it leads to a preferential induction of ISGs and not of IFNβ in response to HCV infection in contrast with the RIG-I/MAVS pathway remains to be determined. Based on our data, we propose now to divide the innate response to acute HCV infection into two phases: an early acute phase in which PKR is activated and a late acute phase that depends on RIG-I, the early phase controlling activation of the late phase. It is now essential to progress towards the generation of specific pharmaceutical inhibitors targeting PKR in order to abrogate the early acute phase to the benefit of the RIG-I-driven late phase. In a more general view, care should now be taken in the choice of compounds designed to be used as immune adjuvants, such as to be devoid of activation of the early acute PKR phase. This will ensure their efficiency as to activate properly the innate immune response through the late acute RIG-I phase.

Methods

Cell cultures and viruses

The culture of Huh7, Huh7.5, Huh7.25.CD81 cells, the preparation of Sendai virus stocks (≈2000 HAU/ml) and of HCV JFH1 stocks (≈6.10^4 FFU/mL and ≈6.10^6 FFU/mL) was as described [8,47]. Preparation and cultures of human primary hepatocytes was as described [48]. Of note, the ability of the Huh7.25.CD81 cells to induce IFN in response to SeV without prior IFN treatment (40-fold) was not observed in our previous study [8].The ability of Sendai virus to induce IFN is related to the presence of copyback DI (Defective Interfering) genomes [49]. The higher IFN inducing ability of the novel Sendai virus stock may have come from an important accumulation of these copyback DI genomes, during its growth in chicken eggs.

PKR inhibitors

The C16 compound [50] and the cell-permeable PRI peptide [51] were provided by Jacques Hugon. These drugs were applied (200 nM for C16 and 30 mM for PRI) one hour before the end of the 2 hr- incubation time with JFH1 and re-added to the medium after washing the cells with phosphate buffered saline (PBS). Note that PRI loses its effect very rapidly, probably through degradation in the cells, and requires to be added every hour to the cells until the end of treatment.

Expression vectors

TRIM25 was cloned from the IFN-treated Huh7.25CD81 cells (500 U/ml IFN-α2a; Cellsciences) after RT-PCR using the forward: 5′-ATGGCAGAGCTGTGCCCCCT-3′ and reverse 5′-CTACTTGGGGGAGCAGATGG-3′ primers. The pcDNA3.1(+) vector expressing 5′HA tagged-TRIM25 (provided by D. Garcin; University of Geneva, Switzerland) was used to generate the TRIM25 $P_{358}L$ construct by site-directed mutagenesis. The

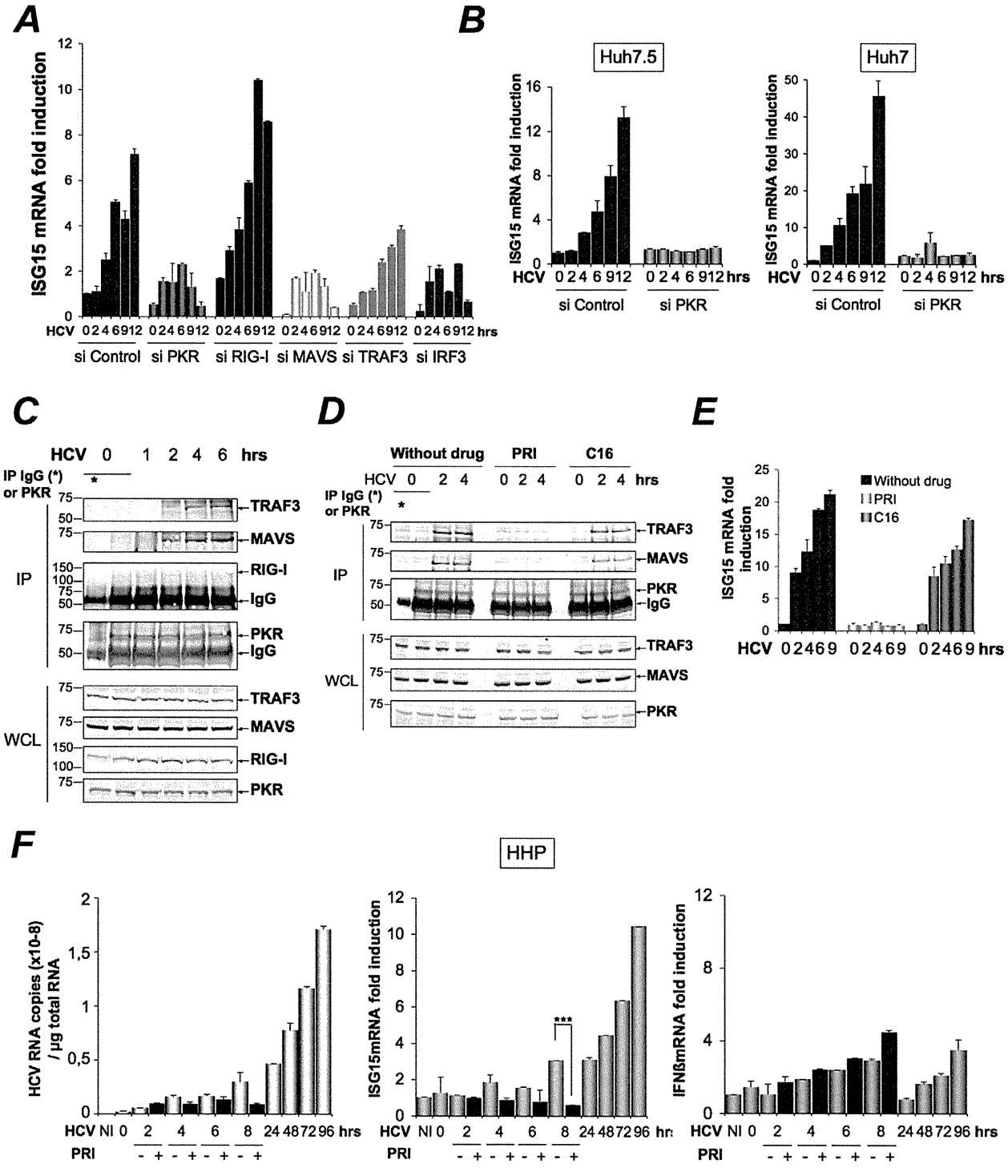

Figure 5. HCV-dependent induction of ISG15 involves PKR, MAVS and TRAF3 and not RIG-I. (**A–B**). **A**-The Huh7.25.CD81 cells were transfected with 50 nM Control siRNA and the different Smartpool siRNAs (50 nM siPKR; 10 nM siRIG-I; 5 nM siMAVS; 50 nM siTRAF3; 50 nM siIRF3) for 48 hrs and infected with JFH1 (m.o.i = 6). (**B**) Huh7.5 or Huh7 cells were transfected with siRNA Control or siPKR (50 nM) for 48 hrs and infected with JFH1 (m.o.i = 0.2 for Huh7.5 or 10 for Huh7). At the times indicated, expression of endogenous ISG15 was determined by RTqPCR and expressed as fold induction. Error bars represent the mean ±S.D for triplicates. The expression level of ISG15 RNA at the start of infection in the siControl cells was 9.97×10^4 copies (Huh7.25.CD81), 1.31×10^4 copies (Huh7.5) and 1.28×10^4 (Huh7). (**C–D**) Huh7.25.CD81 cells, in 100 cm^2 plates, were infected with JFH1 (m.o.i = 0.2) alone (**C**) or in presence of PRI or C16 (**D**). At the times indicated, cell extracts (3.5 mg) were processed for immunoprecipitation of PKR or for incubation with mouse IgG as a control of specificity (asterisk). The detection of the proteins in the complexes and in the whole cell extracts (WCE) was revealed by immunoblot using the Odyssey procedure. (**E**) The Huh7.25.CD81 cells were incubated with PRI or C16 and infected with JFH1 (m.o.i = 0.2) for the times indicated. Expression of endogenous ISG15 was determined as in A–B. The ISG15 RNA levels were 3.81×10^4 copies in the siControl cells. (**F**) Human primary hepatocytes (HHP) were infected with JFH1 (m.o.i = 6). One set of cells was incubated with 30 mM of the PRI inhibitor during 8 hours. At the times indicated, expression of HCV RNA, ISG15 and IFNβ was determined by RTqPCR. The expression levels of ISG15 and IFNβ RNA at the start of infection was 1.05×10^5 copies and $1{,}11\times10^4$ copies, respectively. Inhibition of induction of ISG15 by PRI at 8 hr post-infection was statistically significant (***; p = 0.0001).

doi:10.1371/journal.ppat.1002289.g005

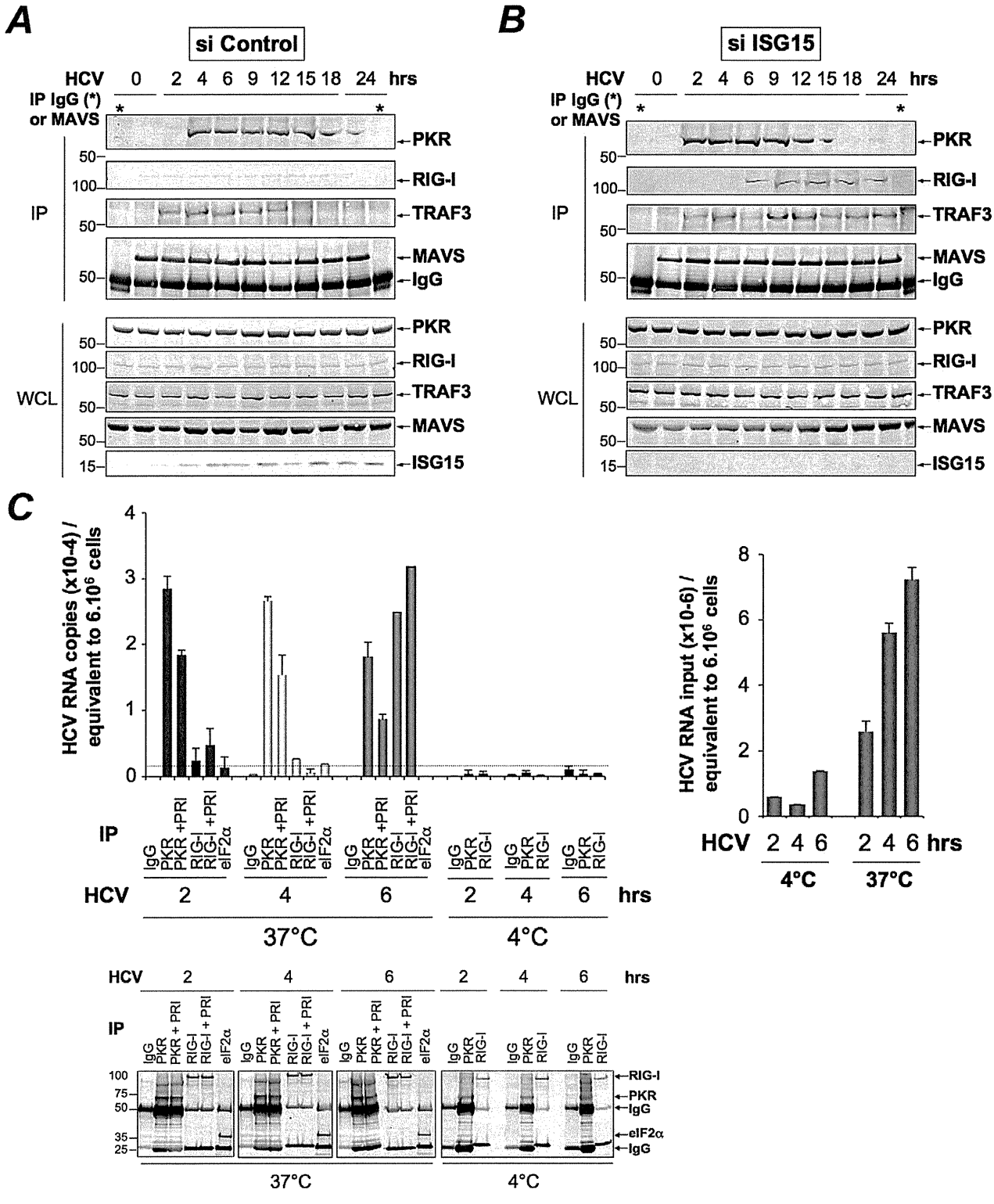

Figure 6. PKR both interacts with MAVS and TRAF3 and binds HCV RNA ahead of RIG-I. (**A–B**)- Huh7.25.CD81 cells were transfected with 25 nM of siRNA Control (**A**) or 25 nM of siRNA ISG15 (**B**) for 48 hrs and infected with JFH1 (m.o.i = 0.2). At the times indicated, cell extracts (4.5 mg) were incubated with anti-MAVS antibodies. In addition, cell extracts prepared at 0 hr post-infection were incubated with mouse IgG as a control of specificity (asterisk). The immunoprecipitated complexes were run on three different NuPAGE gels and blotted using Mab 71/10, anti-MAVS, anti-RIG-I or anti-TRAF3 antibodies. The expression level of each protein was controlled in the total cell extracts. (**C**)- Huh7.25.CD81 cells were incubated with JFH1 (m.o.i = 6) for 2 hrs at 37°C or at 4°C in the absence or presence of 30 μM of PRI. This drug was applied one hour before the end of the incubation time. After washing the cells twice with PBS, the cells were further incubated for 2, 4 or 6 hrs at 37°C or at 4°C in the absence or presence of PRI (added every hour). The cell extracts were processed for crosslinking of RNA to proteins before lysis, as described in Materials and Methods and different immunoprecipitations were performed with antibodies directed against PKR, RIG-I or eIF2α. After extensive washing, the presence of HCV RNA linked to the immunocomplexes was analysed by RTqPCR and the presence of the proteins was verified by Western blot. Measure of HCV RNA in

the cell extracts allowed to estimate its percentage of binding to PKR as 1.09%, 0.47% and 0.25% at 2, 4 and 6 hrs post-infection respectively, and its percentage of binding to RIG-I as 0.34% at 6 hrs post-infection.
doi:10.1371/journal.ppat.1002289.g006

IFNβ-firefly luciferase (pGL2-IFNβ) and pRL-TK Renilla-luciferase reporter plasmids were described previously [8]. The pGL3 luciferase reporter construct containing the −3 to −654 nucleotides of the ISG56 promoter was provided by N.Grandvaux [52]. The Myc-HIS-Ubiquitin construct was provided by R.Kopito (Stanford University, CA). ISG15 was cloned from IFN-treated Huh7 cells using the forward: 5′- GGATCCCATGGGCT-GGGACCTGACGGTG-3′ and reverse 5′-CTCGAGCTCC-GCCCGCCAGGCTCTGT-3′ primers and inserted into the pcDNA3.1(+)HA vector. The Ube1L, UbcH8 and HERC5 constructs were kindly provided by Jon M. Huibregtse [35]. The pcDNA1/AMP vector expressing PKR has been described previously [53].

RNA-mediated interference

The siRNAs directed against PKR, MAVS, RIG-I, TRAF3 and IRF3 which were used for the experiment described in figure 5A correspond to pools of siRNA (Smartpool) obtained from Dharmacon Research, Inc. (Lafayette, CO), as well as siRNAs directed against Ube1L used in Figure 2B. Control (scrambled) siRNA and siRNA directed against PKR or ISG15, used in all other experiments, were chemically synthesized by Dharmacon

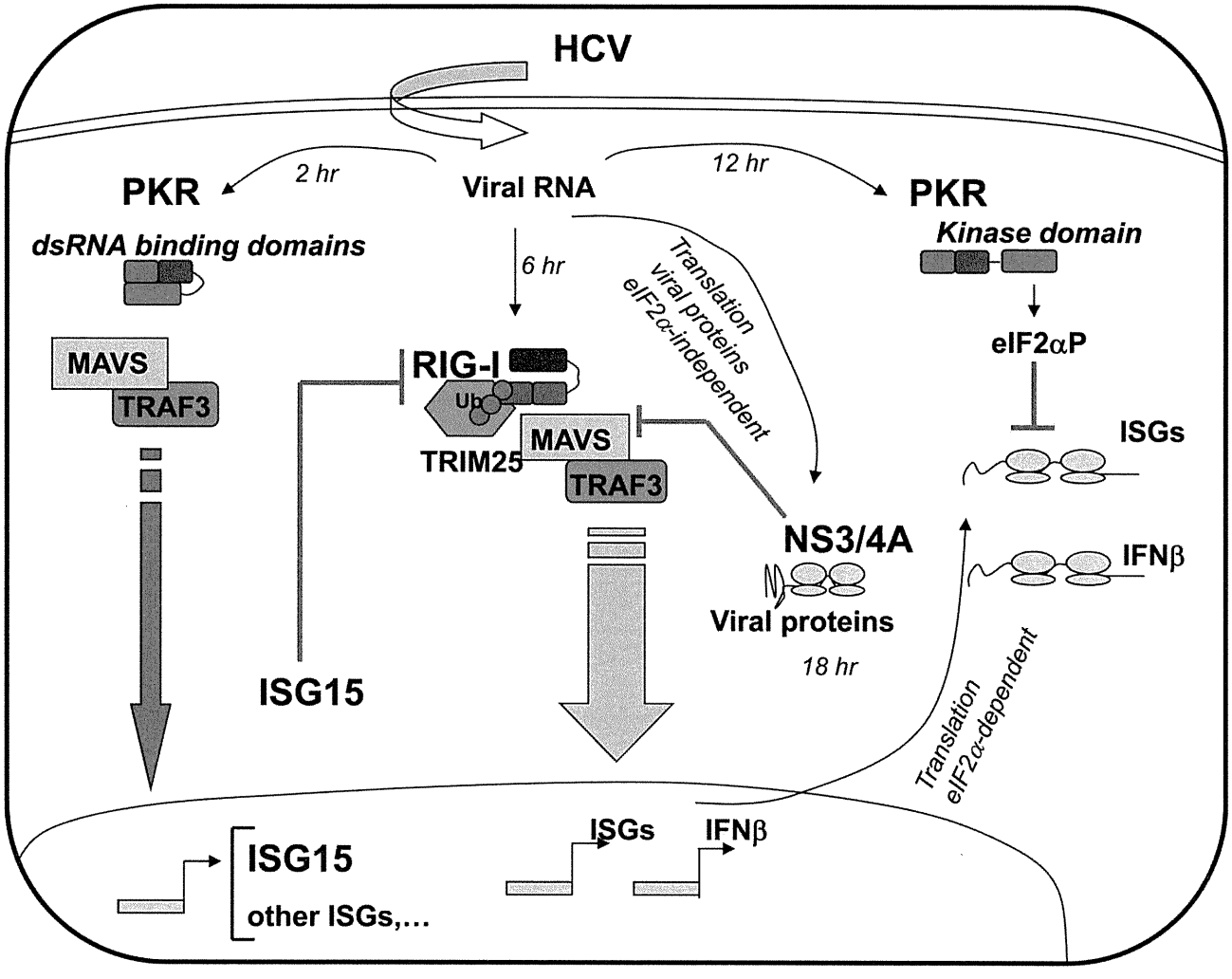

Figure 7. Multiple levels of control of IFN induction during HCV infection. Soon after infection, the HCV RNA is detected by the dsRNA binding domains (DRBD) of PKR ahead (2 hr) of its recognition by the RNA helicase RIG-I (6 hr). Recruitment of PKR by HCV triggers a signaling pathway that involves PKR as an adapter protein to recruit MAVS and TRAF3. This leads to a strong induction of the di-ubiquitine like protein ISG15 as well as other IRF3-dependent ISGs (Interferon-Stimulated Genes). ISG15 negatively controls the TRIM25-mediated ubiquitination (Ub) of RIG-I through an ISGylation process and thus interferes with the ability of RIG-I to recruit its downstream partners, including MAVS and TRAF3, and to induce IFNβ and ISGs. As the infection proceeds, HCV activates the eIF2α kinase function of PKR (12 hr). This leads to a transient (few hours) inhibition of general translation, including that of IFN [8] and ISGs [9] while the eIF2α-independent translation of the viral proteins proceeds unabated. At later times in the infection (18 hr), additional control of IFN induction occurs through cleavage of MAVS by the HCV NS3/4A protease, once the viral proteins have sufficiently accumulated in the cytosol [7,27].
doi:10.1371/journal.ppat.1002289.g007

(scrambled and PKR) and by EUROFINS MWG Operon (ISG15) (Text S1). The siRNAs (final concentration 25 nM or 50 nM) were transfected for 48 h using jetPRIME reagent according to the manufacturer's instructions (PolyPlus transfection TM) before transfection with other plasmids or before infection.

Antibodies

Mab to ISG15 (clone 2.1) was a kind gift of E.Borden [54]. Mab to PKR was produced from the murine 71/10 hybridoma (Agrobio; Fr) with kind permission of A.G.Hovanessian [55]. Other antibodies were as follows: anti-mouse IgG (Santa Cruz), anti-TRAF3 (Santa Cruz), pThr451-PKR (Alexis), MAVS (Alexis), anti-actin (Sigma), anti-pSer10-Histone H3 (Millipore), anti-HCV NS3 (Chemicon), anti-HCV core (Thermo scientific), anti-RIG-I (Alexis Biochemical Inc.), anti-TRIM25 (6105710; BD Bioscience), anti-IRF3 (Santa Cruz), anti-HA (12CA5; Roche) and anti-Myc (Santa Cruz).

Reporter assays

Huh7.25.CD81 cells (80,000 cells/well; 24-well plates) were transfected with 40 ng of pRL-TK Renilla-luciferase reporter (Promega) and 150 ng of either pGL2-IFNβ-Firefly luciferase reporter or pISG56-luciferase reporter and processed for dual-luciferase reporter assay as reported previously [8].

Real-time RT-PCR analysis

Total cellular RNA was extracted using the TRIZOL reagent (Invitrogen). HCV RNA was quantified by one-step RTqPCR. Reverse-transcription, amplification and real-time detection of PCR products were performed with 5 µl total RNA samples, using the SuperScript III Platinum one-step RTqPCR kit (Invitrogen) and an AbiPrism 7700 machine. For the sequence of the different primers, see Text S1. The results were normalized to the amount of cellular endogenous GAPDH RNA using the GAPDH control kit from EuroGentec. Copies number of HCV RNA may vary due to internal calibration and depending on the preparation of the viral stocks. All m.o.i were calculated using the titers expressed in FFU/ml. The IFNβ, ISG15, ISG56, Ube1L and GAPDH amplicons were quantified by a two-step RTqPCR assay as described [8].

Transcriptome analysis

Cellular RNA was extracted and purified from the cells using RNAeasy mini kit (QIAGEN K.K., Tokyo, Japan). Comprehensive DNA microarray analysis was performed with 3D-Gene Human Oligo chip25k with 2-color fluorescence method by New Frontiers Research Laboratories, Toray Industries Inc, Kamakura, Japan as previously described [56]. In brief, each sample was hybridized with 3D-Gene chip. Hybridization signals were scanned using Scan Array Express (PerkinElmer, Waltham, MA). The scanned image was analyzed using GenePix Pro (MDS Analytical Technologies, Sunnyvale, CA). All the analyzed data were scaled by global normalization.

Immunoprecipitation and immunoblot analysis

Cells were washed once with PBS and scraped into lysis buffer 1 (50 mM TRIS-HCl [pH 7.5], 140 mM NaCl, 5% glycerol, 1% CHAPS) that contained phosphatase and protease inhibitors (Complete, Roche Applied Science). The protein concentration was determined by the Bradford method. For immunoprecipitation, lysates were incubated at 4°C overnight with the primary antibodies as indicated and then in the presence of A/G-agarose beads (Santa Cruz Biotechnology) for 60 minutes. The beads were washed three times, and the precipitated proteins were extracted at 70°C using NuPAGE LDS sample buffer. Protein electrophoresis was performed on NuPAGE 4–12% Bis TRIS gels (Invitrogen). Proteins were transferred onto nitrocellulose membranes (Biorad), and probed with specific antibodies. Fluorescent immunoblot images were acquired and quantified by using an Odyssey scanner and the Odyssey 3.1 software (Li-Cor Biosciences) as described previously [8]. For detection of ISG15, cells were lysed in RIPA buffer (50 mM TRIS-HCl [pH 8.0]; 200 mM NaCl; 1% NP-40; 0.5% Sodium Deoxycholate; 0.05% SDS; 2 mM EDTA) and protein electrophoresis was performed on 4–20% polyacrylamide gels (PIERCE).

Nuclear/cytoplasmic extract

Pellets from cells washed in ice-cold phosphate-buffered saline (PBS) were lysed in ice-cold cytoplasmic buffer (10 mM TRIS [pH 8.0], 5 mM EDTA, 0.5 mM EGTA, 0.25% Triton X-100) containing phosphatase and protease inhibitors. The suspension was centrifuged for 30 seconds at 14,000 g and the supernatant (cytoplasmic fraction) was transferred into microcentrifuge tubes. The nuclear pellet was resuspended in Urea buffer (8 M Urea, 10 mM TRIS [pH 7,4], 1 mM EDTA, 1 mM dithiothreitol) containing phosphatase and protease inhibitors, homogenized by vortex and boiled for 10 minutes. The protein concentration was determined by the Bradford method.

Ubiquitination assay

Huh7.25.CD81 cells were transfected for 48 hrs with 5 µg of Myc-His-Ubiquitin expression plasmid using jetPRIME reagent. The cells were then washed in ice-cold PBS containing 20 mM N-ethylmaleimide (Sigma-Aldrich), harvested directly in Gua8 buffer (6 M guanidine-HCl, 300 mM NaCl, 50 mM Na_2HPO_4, 50 mM NaH_2PO_4 [pH 8.0]), briefly sonicated, and centrifuged at 14,000 g for 15 min at 4°C. 1/10th of the lysate was subjected to precipitation with 10% trichloroacetic acid for protein analysis in whole cell extracts. The rest of the lysate was incubated for 2 hrs with 20 µl (packed volume) of Talon resin Ni-affinity beads (Clontech) on a rotating wheel. Bound proteins were washed four times in Gua8 buffer, three times in Urea 6.3 buffer (8 M Urea, 10 mM TRIS, 0.1 M Na_2HPO_4, 20 mM Imidazole [pH 6.3]), and three times in cold PBS, after which they were eluted by boiling in NuPAGE LDS sample buffer. Electrophoresis was performed on 4–12% of acrylamide NuPAGE gels (Invitrogen).

Co-precipitation protein/HCV RNA

Huh7.25.CD81 cells were incubated for 10 min in their culture medium containing 1/10 volume (Vol) of a crosslinking solution (11% Formaldehyde, 0.1 M NaCl, 1 mM Na-EDTA-[pH 8], 0.5 mM Na-EGTA-[pH 8], 50 mM HEPES [pH 8]). The reaction was stopped by addition of a solution of 0.125 M glycine in PBS [pH 8] at room temperature (RT). The cells were washed three times in ice-cold PBS containing 1000 U/ml of RNAse inhibitor (Promega), scraped in PBS and dispatched into three sets containing ½ (set 1), ¼ (set 2) and ¼ (set 3) of the cell suspension. The three sets were centrifuged for 30 seconds at 14,000 g and 4°C and the cell pellets were lysed into lysis buffer 1 containing phosphatase/protease and RNAse inhibitors (Promega) for sets 1 and 2 or into TRIZOL reagent for set 3. Cell lysates from sets 1 and 2 were then incubated at 4°C, first overnight with the appropriate primary antibodies and for 60 minutes in the presence of A/G-agarose beads (Santa Cruz Biotechnology). After the incubation period, the beads were washed four times with buffer 1. Set 1 (HCV RNA bound to immunocomplexes) and set 3 (input HCV RNA) were submitted to TRIZOL treatment and HCV

RNA was quantified by one-step RTqPCR as described previously. The immunoprecipitated proteins from set 2 were extracted at 70°C using NuPAGE LDS sample buffer and analysed by immunoblot after electrophoresis on 4–12% of acrylamide NuPAGE gels (Invitrogen).

Supporting Information

Figure S1 Efficient induction of TRIM25 by IFN in the Huh7.25.CD81 cells. Huh7.25.CD81 cells, seeded at 8×10^4 cells in 24-well plates containing coverslips, were treated with 500 U/ml of IFNα for 24 hrs (IFN) or left untreated (Cont). Cells were fixed with 4% PFA and TRIM25 was detected using anti-TRIM25 antibodies (red). Nuclei are shown in blue after DAPI labelling. Microscope magnification was ×63.
(PDF)

Figure S2 HCV controls RIG-I ubiquitination through ISG15 in the Huh7 cells. Huh7 cells were transfected for 24 hrs with 25 nM of siRNA (Control or ISG15) and for another 24 hr with 5 µg of a His-Myc-Ubiquitin plasmid in absence or presence of 5 µg of a plasmid expressing HA-TRIM25. The cells were infected with JFH1 (m.o.i = 0.2). At the times indicated, cell extracts were processed for analysis of RIG-I ubiquitination and the expression of the different proteins in the total cell extracts. Efficiency of infection by JFH1 in the Huh7 cells was 2 log less than in the Huh7.25.CD81 cells.
(PDF)

Figure S3 Expression of ISG15 and ISG15 conjugating enzymes inhibit IFN induction in response to SeV. Huh7.25.CD81 cells were transfected with a plasmid expressing HA-ISG15 alone or in the presence of plasmids expressing the ISG15 conjugating enzymes Ube1L (E1), UbcH8 (E2) and HERC5 (E3). The cells were then infected with JFH1 (m.o.i = 6) for the times indicated. Stimulation of endogenous IFNβ RNA expression was determined by RTqPCR and expressed as fold induction. The degree of statistical significance is indicated by stars after calculation of the p-values (from left to right: 0.0124 and 0.0058).
(PDF)

Figure S4 Control of efficiency of siRNA Ube1L in the Huh7.25.CD81 cells. The Huh7.25.CD81 cells were transfected with 50 nM of siRNA directed against Ube1L for 48 hours and infected with HCV. RNA was prepared from the cells at different times post infection as indicated and expression levels of Ube1L was determined by RTqPCR.
(PDF)

Figure S5 Modulation of PKR activation by ISG15. Huh7.25.CD81 cells, in 100 cm^2 plates, were transfected with siRNA Control or siRNA ISG15 or transfected with a plasmid expressing HA-ISG15 for 48 hrs and infected with JFH1 (m.o.i = 6). At the indicated times post-infection, cell extracts (2.2 mg) were processed for immunoprecipitation of PKR. The immunoprecipitated complexes were run on two different NuPAGE gels and blotted using Mab 71/10 or anti-phosphorylated PKR antibodies (PKR-P). The presence of PKR and PKR-P was revealed using the Odyssey procedure. The bands corresponding to total PKR and phosphorylated PKR were quantified using the Odyssey software and expressed as the ratio PKR-P/PKR in the absence (siISG15) and in the presence of ISG15 in the control cells (Control) or after transfection of the ISG15 expressing plasmid (HA-ISG15).
(PDF)

Figure S6 Induction of ISG56 by Sendai virus in the Huh7.25.CD81 cells does not depend on PKR. Huh7.25.CD81 cells were either transfected with 25 nM of siRNA Control or 25 nM siPKR for 24 hrs and infected with SeV for the times indicated. The effect of PKR silencing on the stimulation of expression of endogenous ISG56 was determined by RTqPCR and expressed as fold induction. Error bars represent the mean ±S.D for triplicates. The expression levels of ISG56 RNA at the start of infection were respectively 1.15×10^5 copies (siControl) and 1.16×10^5 copies (siPKR).
(PDF)

Figure S7 Control of the efficiency of siRNA treatment in the Huh7.25.CD81 cells. The Huh7.25.CD81 cells were transfected for 48 hrs with 50 nM Control siRNA or with the different Smartpool siRNAs as shown (50 nM siPKR; 10 nM siRIG-I; 50 nM siIRF3; 50 nM siTRAF3; 5 nM siMAVS). Total cell extracts were prepared and the expression level of each protein, as well as that of actin used as control, was revealed by immunoblot and Odyssey procedure after a run on NuPAGE gels. Under each lane, the numbers represent the quantification of the different protein bands performed using the Odyssey software.
(TIF)

Figure S8 HCV triggers nuclear translocation of IRF3 early after infection in the Huh7.25.CD81 cells. Huh7.25.CD81 cells, seeded at 10^5 cells in 24-well plates containing coverslips, were infected for different times (0, 4 and 6 hours) at 37°C with JFH1 (moi = 6) or with SeV (40 HAU/ml) in the absence or in the presence of 10 ng/ml Leptomycine B (LB; Sigma), which was used here as a convenient mean to enhance the nuclear detection of IRF3 since it can interfere with nuclear export [57]. Cells were fixed with 4% PFA and IRF3 was detected using anti-IRF3 antibodies (red). Nuclei are shown in blue after DAPI labelling. The arrows show the presence of IRF3 in the nucleus. Microscope magnification was ×63.
(PDF)

Figure S9 Induction of ISG56 by HCV in the Huh7.5 and Huh7 cells depends on PKR. Huh7.5 or Huh7 cells were transfected with siRNA Control or siPKR (50 nM) for 48 hrs and infected with JFH1 (m.o.i = 0.2 for Huh7.5 or 10 for Huh7). At the times indicated, expression of endogenous ISG56 was determined by RTqPCR and expressed as fold induction. Error bars represent the mean ±S.D for triplicates. The expression levels of ISG56 RNA at the start of infection in the siControl cells was 1.37×10^4 copies (Huh7.5 cells) and 1.28×10^4 copies (Huh7 cells).
(PDF)

Figure S10 Induction of ISG56 by HCV is specifically inhibed by the PKR inhibitor PRI. The Huh7.25.CD81 cells were incubated with PRI or C16 and infected with JFH1 (m.o.i = 0.2) for the times indicated. RTqPCR analysis of endogenous ISG56 was determined by RTqPCR and expressed as fold induction. The expression levels of ISG56 RNA at the start of infection in the control cells was 1.97×10^4 copies.
(TIF)

Figure S11 The RNAse inhibitor RNAsin does not favour the formation of a RIG-I/PKR complex upon HCV infection. Two sets of Huh7.25.CD81 cells were plated into 100 cm^2 plates and infected with JFH1. At the times indicated, cell extracts (3.5 mg) from the two sets were processed similarly for immunoprecipitation of PKR or for incubation with mouse IgG as a control of specificity (asterisk), except that care was taken to add the RNAse inhibitor RNAsin (1000 U/ml) at all steps for the second set (+RNAsin). Detection of RIG-I, MAVS, and PKR in

the complexes and in the whole cell extracts (WCE) was revealed by immunoblot using the Odyssey procedure. Detection of Actin in WCE served as loading control.
(PDF)

Table S1 Transcriptome analysis of PKR-dependent downpregulated gene upon 12 hrs of HCV infection. Preparation of samples was as described under Table 1. The list shows genes that were affected no more than twice by the depletion of PKR in the control cells (0.5< siPKR mock/siCt <1.6). The dependence of each of these genes in regards with PKR for their inhibition by HCV is expressed as log2 (ratio (siPKR HCV/siCt Mock)−(siCt HCV/siCt Mock) (indicated by log2*) with a cut-off of ≈2.0 fold.
(DOC)

Text S1 Supplementary methods.
(DOC)

Acknowledgments

We thank Michael Gale Jr, Pierre-Olivier Vidalain and Christine Neuveut for critical reviews of the manuscript. We thank Adrien Six, Eric Batsche and Agata Budkowska for discussions. We thank Ernest Borden for the gift of anti-ISG15 antibodies, Jon Huibregste for the gift of plasmids expressing ISG15 conjugating enzymes, Dominique Garcin for providing the Sendai virus, Claire Gondeau and Martine Daujat for their help in the preparation and infection of human primary hepatocytes with JFH1.

Author Contributions

Conceived and designed the experiments: NA TW EFM. Performed the experiments: NA SD DA MF FS-O. Analyzed the data: NA TW EFM. Contributed reagents/materials/analysis tools: JH DA MF FS-O TW. Wrote the paper: NA EFM.

References

1. Gack MU, Shin YC, Joo CH, Urano T, Liang C, et al. (2007) TRIM25 RING-finger E3 ubiquitin ligase is essential for RIG-I-mediated antiviral activity. Nature 446: 916–920.
2. Gack MU, Kirchhofer A, Shin YC, Inn KS, Liang C, et al. (2008) Roles of RIG-I N-terminal tandem CARD and splice variant in TRIM25-mediated antiviral signal transduction. Proc Natl Acad Sci U S A 105: 16743–16748.
3. Yoneyama M, Fujita T (2009) RNA recognition and signal transduction by RIG-I-like receptors. Immunol Rev 227: 54–65.
4. Binder M, Kochs G, Bartenschlager R, Lohmann V (2007) Hepatitis C virus escape from the interferon regulatory factor 3 pathway by a passive and active evasion strategy. Hepatology 46: 1365–1374.
5. Saito T, Owen DM, Jiang F, Marcotrigiano J, Gale M, Jr. (2008) Innate immunity induced by composition-dependent RIG-I recognition of hepatitis C virus RNA. Nature 454: 523–527.
6. Sumpter R, Jr., Loo YM, Foy E, Li K, Yoneyama M, et al. (2005) Regulating intracellular antiviral defense and permissiveness to hepatitis C virus RNA replication through a cellular RNA helicase, RIG-I. J Virol 79: 2689–2699.
7. Meylan E, Curran J, Hofmann K, Moradpour D, Binder M, et al. (2005) Cardif is an adaptor protein in the RIG-I antiviral pathway and is targeted by hepatitis C virus. Nature 437: 1167–1172.
8. Arnaud N, Dabo S, Maillard P, Budkowska A, Kalliampakou KI, et al. (2010) Hepatitis C virus controls interferon production through PKR activation. PLoS One 5: e10575.
9. Garaigorta U, Chisari FV (2009) Hepatitis C virus blocks interferon effector function by inducing protein kinase R phosphorylation. Cell Host Microbe 6: 513–522.
10. Mihm S, Frese M, Meier V, Wietzke-Braun P, Scharf JG, et al. (2004) Interferon type I gene expression in chronic hepatitis C. Lab Invest 84: 1148–1159.
11. Sarasin-Filipowicz M, Oakeley EJ, Duong FH, Christen V, Terracciano L, et al. (2008) Interferon signaling and treatment outcome in chronic hepatitis C. Proc Natl Acad Sci U S A 105: 7034–7039.
12. Bigger CB, Guerra B, Brasky KM, Hubbard G, Beard MR, et al. (2004) Intrahepatic gene expression during chronic hepatitis C virus infection in chimpanzees. J Virol 78: 13779–13792.
13. Takahashi K, Asabe S, Wieland S, Garaigorta U, Gastaminza P, et al. (2010) Plasmacytoid dendritic cells sense hepatitis C virus-infected cells, produce interferon, and inhibit infection. Proc Natl Acad Sci U S A 107: 7431–7436.
14. Askarieh G, Alsio A, Pugnale P, Negro F, Ferrari C, et al. (2010) Systemic and intrahepatic interferon-gamma-inducible protein 10 kDa predicts the first-phase decline in hepatitis C virus RNA and overall viral response to therapy in chronic hepatitis C. Hepatology 51: 1523–1530.
15. Asselah T, Bieche I, Narguet S, Sabbagh A, Laurendeau I, et al. (2008) Liver gene expression signature to predict response to pegylated interferon plus ribavirin combination therapy in patients with chronic hepatitis C. Gut 57: 516–524.
16. Chen L, Borozan I, Feld J, Sun J, Tannis LL, et al. (2005) Hepatic gene expression discriminates responders and nonresponders in treatment of chronic hepatitis C viral infection. Gastroenterology 128: 1437–1444.
17. Chen L, Sun J, Meng L, Heathcote J, Edwards A, et al. (2010) ISG15, a ubiquitin-like interferon stimulated gene, promotes Hepatitis C Virus production in vitro: Implications for chronic infection and response to treatment. J Gen Virol 91: 382–388.
18. Kim MJ, Hwang SY, Imaizumi T, Yoo JY (2008) Negative feedback regulation of RIG-I-mediated antiviral signaling by interferon-induced ISG15 conjugation. J Virol 82: 1474–1483.
19. Akazawa D, Date T, Morikawa K, Murayama A, Miyamoto M, et al. (2007) CD81 expression is important for the permissiveness of Huh7 cell clones for heterogeneous hepatitis C virus infection. J Virol 81: 5036–5045.
20. Nisole S, Stoye JP, Saib A (2005) TRIM family proteins: retroviral restriction and antiviral defence. Nat Rev Microbiol 3: 799–808.
21. Zou W, Wang J, Zhang DE (2007) Negative regulation of ISG15 E3 ligase EFP through its autoISGylation. Biochem Biophys Res Commun 354: 321–327.
22. Jeon YJ, Yoo HM, Chung CH (2010) ISG15 and immune diseases. Biochim Biophys Acta 1802: 485–496.
23. Kim KI, Yan M, Malakhova O, Luo JK, Shen MF, et al. (2006) Ube1L and protein ISGylation are not essential for alpha/beta interferon signaling. Mol Cell Biol 26: 472–479.
24. Chen WH, Basu S, Bhattacharjee AK, Cross AS (2010) Enhanced antibody responses to a detoxified lipopolysaccharide-group B meningococcal outer membrane protein vaccine are due to synergistic engagement of Toll-like receptors. Innate Immun 16: 322–332.
25. Broering R, Zhang X, Kottilil S, Trippler M, Jiang M, et al. (2010) The interferon stimulated gene 15 functions as a proviral factor for the hepatitis C virus and as a regulator of the IFN response. Gut 59: 1111–1119.
26. Elco CP, Guenther JM, Williams BRG, Sen GC (2005) Analysis of genes induced by Sendai virus infection of mutant cell lines reveals essential roles of interferon regulatory factor 3, NF-kappaB, and interferon but not toll-like receptor 3. J Virol 79: 3920–3929.
27. Loo YM, Owen DM, Li K, Erickson AK, Johnson CL, et al. (2006) Viral and therapeutic control of IFN-beta promoter stimulator 1 during hepatitis C virus infection. Proc Natl Acad Sci U S A 103: 6001–6006.
28. Bigger CB, Brasky KM, Lanford RE (2001) DNA microarray analysis of chimpanzee liver during acute resolving hepatitis C virus infection. J Virol 75: 7059–7066.
29. Farell PJ, Broeze RJ, Lengyel P (1979) Accumulation of an mRNA and protein in interferon-treated Ehrlich ascites tumour cells. Nature (London) 279: 523–524.
30. Haas AL, Ahrens P, Bright PM, Ankel H (1987) Interferon induces a 15-kilodalton protein exhibiting marked homology to ubiquitin. J Biol Chem 262: 11315–11323.
31. Zhao C, Denison C, Huibregtse JM, Gygi S, Krug RM (2005) Human ISG15 conjugation targets both IFN-induced and constitutively expressed proteins functioning in diverse cellular pathways. Proc Natl Acad Sci U S A 102: 10200–10205.
32. Yuan W, Krug RM (2001) Influenza B virus NS1 protein inhibits conjugation of the interferon (IFN)-induced ubiquitin-like ISG15 protein. Embo J 20: 362–371.
33. Wong JJ, Pung YF, Sze NS, Chin KC (2006) HERC5 is an IFN-induced HECT-type E3 protein ligase that mediates type I IFN-induced ISGylation of protein targets. Proc Natl Acad Sci U S A 103: 10735–10740.
34. Zou W, Zhang DE (2006) The interferon-inducible ubiquitin-protein isopeptide ligase (E3) EFP also functions as an ISG15 E3 ligase. J Biol Chem 281: 3989–3994.
35. Durfee LA, Lyon N, Seo K, Huibregtse JM (2010) The ISG15 conjugation system broadly targets newly synthesized proteins: implications for the antiviral function of ISG15. Mol Cell 38: 722–732.
36. Wieland SF, Chisari FV (2005) Stealth and cunning: hepatitis B and hepatitis C viruses. J Virol 79: 9369–9380.
37. Jiang J, Tang H (2010) Mechanism of inhibiting type I interferon induction by hepatitis B virus×protein. Prein Cell 1: 1106–1117.
38. Wei C, Ni C, Song T, Liu Y, Yang X, et al. (2010) The hepatitis B virus×protein disrupts innate immunity by downregulating mitochondrial antiviral signaling protein. J Immunol 185: 1158–1168.
39. Chen GG, Lai PB, Ho RL, Chan PK, Xu H, et al. (2004) Reduction of double-stranded RNA-activated protein kinase in hepatocellular carcinoma associated with hepatitis B virus. J Med Virol 73: 187–194.

40. Shimoike T, McKenna SA, Lindhout DA, Puglisi JD (2009) Translational insensitivity to potent activation of PKR by HCV IRES RNA. Antiviral Res 83: 228–237.
41. Nallagatla SR, Hwang J, Toroney R, Zheng X, Cameron CE, et al. (2007) 5′-triphosphate-dependent activation of PKR by RNAs with short stem-loops. Science 318: 1455–1458.
42. Gil J, Garcia MA, Gomez-Puertas P, Guerra S, Rullas J, et al. (2004) TRAF family proteins link PKR with NF-kappa B activation. Mol Cell Biol 24: 4502–4512.
43. Oganesyan G, Saha SK, Guo B, He JQ, Shahangian A, et al. (2006) Critical role of TRAF3 in the Toll-like receptor-dependent and -independent antiviral response. Nature 439: 208–211.
44. Zhang P, Samuel CE (2008) Induction of protein kinase PKR-dependent activation of interferon regulatory factor 3 by vaccinia virus occurs through adapter IPS-1 signaling. J Biol Chem 283: 34580–34587.
45. McAllister CS, Samuel CE (2009) The RNA-activated protein kinase enhances the induction of interferon-beta and apoptosis mediated by cytoplasmic RNA sensors. J Biol Chem 284: 1644–1651.
46. McAllister CS, Toth AM, Zhang P, Devaux P, Cattaneo R, et al. (2010) Mechanisms of protein kinase PKR-mediated amplification of beta interferon induction by C protein-deficient measles virus. J Virol 84: 380–386.
47. Strahle L, Marq JB, Brini A, Hausmann S, Kolakofsky D, et al. (2007) Activation of the beta interferon promoter by unnatural Sendai virus infection requires RIG-I and is inhibited by viral C proteins. J Virol 81: 12227–12237.
48. Biron-Andreani C, Raulet E, Pichard-Garcia L, Maurel P (2010) Use of human hepatocytes to investigate blood coagulation factor. Methods Mol Biol 640: 431–445.
49. Strahle L, Garcin D, Kolakofsky D (2006) Sendai virus defective-interfering genomes and the activation of interferon-beta. Virology 351: 101–111.
50. Jammi NV, Whitby LR, Beal PA (2003) Small molecule inhibitors of the RNA-dependent protein kinase. Biochem Biophys Res Commun 308: 50–57.
51. Nekhai S, Bottaro DP, Woldehawariat G, Spellerberg A, Petryshyn R (2000) A cell-permeable peptide inhibits activation of PKR and enhances cell proliferation. Peptides 21: 1449–1456.
52. Grandvaux N, Servant MJ, tenOever B, Sen GC, Balachandran S, et al. (2002) Transcriptional profiling of interferon regulatory factor 3 target genes: direct involvement in the regulation of interferon-stimulated genes. J Virol 76: 5532–5539.
53. Bonnet MC, Daurat C, Ottone C, Meurs EF (2006) The N-terminus of PKR is responsible for the activation of the NF-kappaB signaling pathway by interacting with the IKK complex. Cell Signal 18: 1865–1875.
54. Malakhov MP, Kim KI, Malakhova OA, Jacobs BS, Borden EC, et al. (2003) High-throughput immunoblotting. Ubiquitiin-like protein ISG15 modifies key regulators of signal transduction. J Biol Chem 278: 16608–16613.
55. Laurent AG, Krust B, Galabru J, Svab J, Hovanessian AG (1985) Monoclonal antibodies to interferon induced 68,000 Mr protein and their use for the detection of double-stranded RNA dependent protein kinase in human cells. Proc Natl Acad SciUSA 82: 4341–4345.
56. Iwano S, Ichikawa M, Takizawa S, Hashimoto H, Miyamoto Y (2010) Identification of AhR-regulated genes involved in PAH-induced immunotoxicity using a highly-sensitive DNA chip, 3D-Gene Human Immunity and Metabolic Syndrome 9k. Toxicol In Vitro 24: 85–91.
57. Wolff B, Sanglier JJ, Wang Y (1997) Leptomycin B is an inhibitor of nuclear export: inhibition of nucleo-cytoplasmic translocation of the human immunodeficiency virus type 1 (HIV-1) Rev protein and Rev-dependent mRNA. Chem Biol 4: 139–147.

THE JOURNAL OF BIOLOGICAL CHEMISTRY VOL. 286, NO. 43, pp. 37264–37273, October 28, 2011

Role of the Endoplasmic Reticulum-associated Degradation (ERAD) Pathway in Degradation of Hepatitis C Virus Envelope Proteins and Production of Virus Particles*[S]

Received for publication, May 7, 2011, and in revised form, August 18, 2011 Published, JBC Papers in Press, August 30, 2011, DOI 10.1074/jbc.M111.259085

Mohsan Saeed[§], Ryosuke Suzuki[‡], Noriyuki Watanabe[‡], Takahiro Masaki[‡], Mitsunori Tomonaga[‡], Amir Muhammad[¶], Takanobu Kato[‡], Yoshiharu Matsuura[‖], Haruo Watanabe[§], Takaji Wakita[‡], and Tetsuro Suzuki[‡‡‡1]**

*From the [‡]Department of Virology II, National Institute of Infectious Diseases, Tokyo 162-8640, Japan, the [§]Department of Infection and Pathology, Graduate School of Medicine, the University of Tokyo, Tokyo 113-0033, Japan, the [¶]Department of Pathology, Khyber Girls Medical College, Peshawar 25000, Pakistan, the [‖]Research Institute of Microbial Diseases, Osaka University, Osaka 565-0871, Japan, the **National Institute of Infectious Diseases, Tokyo 162-8640, Japan, and the [‡‡‡]Department of Infectious Diseases, Hamamatsu University School of Medicine, Hamamatsu 431-3192, Japan*

Background: HCV causes ER stress in the infected cells.
Results: HCV-induced ER stress leads to increased expression of certain proteins that in turn enhance the degradation of HCV glycoproteins and decrease production of virus particles.
Conclusion: HCV infection activates the ERAD pathway, leading to modulation of virus production.
Significance: ERAD plays a crucial role in the viral life cycle.

Viral infections frequently cause endoplasmic reticulum (ER) stress in host cells leading to stimulation of the ER-associated degradation (ERAD) pathway, which subsequently targets unassembled glycoproteins for ubiquitylation and proteasomal degradation. However, the role of the ERAD pathway in the viral life cycle is poorly defined. In this paper, we demonstrate that hepatitis C virus (HCV) infection activates the ERAD pathway, which in turn controls the fate of viral glycoproteins and modulates virus production. ERAD proteins, such as EDEM1 and EDEM3, were found to increase ubiquitylation of HCV envelope proteins via direct physical interaction. Knocking down of EDEM1 and EDEM3 increased the half-life of HCV E2, as well as virus production, whereas exogenous expression of these proteins reduced the production of infectious virus particles. Further investigation revealed that only EDEM1 and EDEM3 bind with SEL1L, an ER membrane adaptor protein involved in translocation of ERAD substrates from the ER to the cytoplasm. When HCV-infected cells were treated with kifunensine, a potent inhibitor of the ERAD pathway, the half-life of HCV E2 increased and so did virus production. Kifunensine inhibited the binding of EDEM1 and EDEM3 with SEL1L, thus blocking the ubiquitylation of HCV E2 protein. Chemical inhibition of the ERAD pathway neither affected production of the Japanese encephalitis virus (JEV) nor stability of the JEV envelope protein. A co-immunoprecipitation assay showed that EDEM orthologs do not bind with JEV envelope protein. These findings highlight the crucial role of the ERAD pathway in the life cycle of specific viruses.

Quality control of proteins, such as the elimination of misfolded proteins, is largely connected with the endoplasmic reticulum (ER),[2] which is an organelle responsible for the folding and distribution of secretory proteins to their sites of action. This pathway is termed ER-associated degradation (ERAD) and is triggered by ER stress. It results in retrotranslocation of misfolded proteins into the cytosol, followed by polyubiquitylation and proteasomal degradation (1). Several viral infections have been reported to trigger the ERAD pathway (2–4); however, the role of this pathway in the life cycle of viruses remains poorly defined.

Initiation of the ERAD pathway occurs from the oligomerization and autophosphorylation of IRE1, an ER stress sensor. The activated IRE1 removes an intron from X-box-binding protein 1 (XBP1) mRNA, which then encodes a potent transcription factor for activation of genes, for example, ER degradation-enhancing α-mannosidase-like protein (EDEM). EDEM1 (5), along with its two homologs EDEM2 (6) and EDEM3 (7), as well as ER mannosidase I (ER ManI), belong to the glycoside hydrolase 47 family. EDEMs are thought to function as lectins that deliver misfolded glycoproteins to the ERAD pathway. However, the precise mechanism by which they assist in glycoprotein quality control remains unclear.

Hepatitis C virus (HCV) infection is a major cause of chronic liver disease. The RNA genome of HCV, a member of the Fla-

* This work was supported by grants-in-aid from the Ministry of Health, Labor and Welfare, and from the Ministry of Education, Culture, Sports, Science, and Technology, Japan.
[S] The on-line version of this article (available at http://www.jbc.org) contains supplemental Figs. S1–S7.
[1] To whom correspondence should be addressed: Dept. of Infectious Diseases, Hamamatsu University School of Medicine, Hamamatsu 431-3192, Japan. Tel.: 81-53-435-2336; Fax: 81-53-435-2338; E-mail: tesuzuki@hama-med.ac.jp.

[2] The abbreviations used are: ER, endoplasmic reticulum; CHX, cycloheximide; EDEM, ER degradation-enhancing α-mannosidase-like protein; ERAD, ER-associated degradation; HCV, hepatitis C virus; JEV, Japanese encephalitis virus; KIF, kifunensine; ManI, mannosidase I; m.o.i., multiplicity of infection; TM, tunicamycin; XBP1, X-box-binding protein 1; IRE, inositol-requiring enzyme.

viviridae family, encodes the viral structural proteins Core, E1, E2, and p7, as well as six nonstructural proteins (8, 9). Two *N*-glycosylated envelope proteins E1 and E2 are exposed on the surface of the virus and are necessary for viral entry.

The aim of this study was to investigate whether the ERAD pathway is activated upon HCV infection and whether this affects the quality control of virus glycoproteins and virion production. We show that HCV infection triggers the ERAD pathway, possibly through IRE1-mediated splicing of XBP1. Moreover, EDEM1 and EDEM3, but not EDEM2, interact with HCV glycoproteins, resulting in increased ubiquitylation. EDEM1 knockdown and chemical inhibition of the ERAD pathway increases glycoprotein stability, as well as production of infectious virus particles, whereas overexpression of EDEM1 decreases virion production. These results provide insight into the mechanism by which HCV triggers the ERAD pathway and subsequently affects the quality control of virus glycoproteins and virus particle production.

EXPERIMENTAL PROCEDURES

Cell Culture and Chemicals—Human hepatoma cells HuH-7 and HuH-7.5.1 (a gift from Dr. F. V. Chisari (The Scripps Research Institute) (10) and human embryonic kidney cells 293T were cultured at 37 °C and 5% CO_2 in DMEM containing 10% FBS, 10 mM HEPES, 1 mM sodium pyruvate, nonessential minimum amino acids, 100 units/ml penicillin, and 100 μg/ml streptomycin. Tunicamycin (TM) was purchased from Sigma-Aldrich, and kifunensine (KIF) was purchased from Toronto Research Chemicals (Ontario, Canada).

Preparation of Virus Stock—HCV JFH-1 was generated by introducing *in vitro* transcribed RNA into HuH-7.5.1 cells by electroporation, and virus stocks were prepared by infecting at a multiplicity of infection (m.o.i.) of 0.01, as described previously (10). Infected cells were grown in culture medium containing 2% FBS, and supernatants were collected after multiple passages to get high titer virus. The supernatants were concentrated using a 500-kDa hollow fiber module (GE Healthcare) resulting in ~90% recovery of the virus. Focus-forming units were measured with an anti-HCV core antibody to determine virus titration (2H9, described below). Virus stocks containing 1×10^7 focus-forming units/ml were divided into small aliquots and stored at −80 °C until use. rAT strain of Japanese encephalitis virus (JEV) (11) was used to generate virus stock.

Plasmids—cDNAs of mouse EDEM1-HA, EDEM2, and EDEM3-HA, having 92, 93, and 91% amino acid homology with their human orthologs, respectively, were a kind gift from Drs. N. Hosokawa (Kyoto University) and K. Nagata (Kyoto Sangyo University). A HA tag was attached to the C terminus of EDEM2 by PCR, and sequencing analysis was performed to confirm the sequence. To generate pJFH/E1dTM-myc and pJFH/E2dTM-myc, HCV E1 encoding amino acids 170–352 and HCV E2 encoding amino acids 340–714 of JFH-1 polyprotein were amplified by PCR with forward primer and reverse primer containing NotI and XbaI restriction sites, respectively, and cloned into a NotI/XbaI site of the pEF1/Myc-His plasmid (Invitrogen). The pCAGC105E plasmid carrying PrM and E proteins of the rAT strain of JEV has been described (12). Plasmids carrying the firefly luciferase reporter gene under control of the intact promoter of GRP78 and GRP94 or the defective promoter lacking ERSE elements have been described (13) and were a kind gift from Dr. K. Mori (Kyoto University).

Antibodies—Rabbit polyclonal antibodies included anti-HA (Sigma-Aldrich), anti-HCV NS5A (14), anti-SEL1L (Sigma-Aldrich), anti-ubiquitin (MBL, Nagoya, Japan), and anti-JEV E antibodies. The mouse monoclonal antibodies were anti-HA (clone 16B12; Covance, Emeryville, CA), anti-HCV E2 (clone 8D10-3),[3] anti-β-actin (clone AC15; Sigma-Aldrich), anti-HCV core (clone 2H9) (15), and anti-Myc (clone 9E10; Santa Cruz Biotechnology, Santa Cruz, CA) antibodies. Anti-JEV antibodies have been described (16) and were a kind gift from Drs. C. K. Lim and T. Takasaki (National Institute of Infectious Diseases).

Analysis of XBP1 Splicing—Total RNA was extracted from cells using Isogen (Nippon Gene, Tokyo, Japan) following the manufacturer's protocol, and 2 μg of RNA was subjected to cDNA synthesis using oligo(dT) and Superscript III (Invitrogen). PCR was carried out using specific primers 5′-AAACAGAGTAGCAGCTCAGACTGC-3′ and 5′-GTATCTCTAAGACTAGGGGCTTGGTA-3′ for XBP1 and 5′-TCCTGTGGCATCCACGAAACT-3′ and 5′-GAAGCATTTGCGGTGGACGAT-3′ for β-actin to generate PCR fragments of 598 bp for unspliced XBP1, 572 bp for spliced XBP1, and 315 bp for β-actin. The following cycling conditions were used to amplify the genes: 1 cycle of 98 °C for 3 min, followed by 30 cycles of 98 °C for 20 s, 55 °C for 30 s, and 72 °C for 1 min, followed by a final extension of 72 °C for 10 min. The PCR product of XBP1 was further digested with PstI enzyme (New England Biolabs) and resolved on a 2% agarose gel prepared in TAE buffer. Unspliced XBP1 yielded two smaller fragments of 291 and 307 bp whereas spliced XBP1 stayed intact due to loss of the restriction site after splicing.

Gene Microarray Analysis—For microarray analysis, RNA was extracted from HuH-7.5.1 cells at 48 and 72 h after JFH-1 infection. Cells treated for 12 h with 5 μg/ml TM served as a positive control. Hybridization was performed on a 3D-Gene (see 3D-Gene web site) Human Oligonucleotide chip 25k (Toray Industries Inc., Tokyo, Japan). For efficient hybridization, this microarray chip has three dimensions and is constructed with a well between the probes and cylinder stems with 70-mer oligonucleotide probes on the top. Total RNA was labeled with Cy3 or Cy5 using the Amino Allyl MessageAMP II aRNA Amplification kit (Applied Biosystems). The Cy3- or Cy5-labeled aRNA pools were subjected to hybridization for 16 h using the supplier's protocol. Hybridization signals were scanned using a ScanArray Express Scanner (PerkinElmer Life Sciences) and processed by GenePixPro version 5.0 (Molecular Devices, Sunnyvale, CA). Detected signals for each gene were normalized using a global normalization method (Cy3/Cy5 ratio median = 1). Genes with Cy3/Cy5 normalized ratios $>\log_2 1.0$ or $<\log_2 -1.0$ were defined, respectively, as significantly up- or down-regulated genes.

Quantification of Cellular Gene Expression—Gene expression levels were measured using predesigned assay-on-demand (Applied Biosystems). RT-PCR amplification was performed

[3] D. Akazawa, N. Nakamura, and T. Wakita, unpublished data.

under the following conditions: 48 °C for 30 min, 95 °C for 10 min, 50 cycles of 95 °C for 15 s, and 60 °C for 1 min. Standard curves were constructed on a 1:5 serial dilution of the RNA template. The results were normalized to GAPDH mRNA levels.

Determination of Protein Stability—HuH-7 cells were infected with HCV JFH-1 at a m.o.i. of 2. Six hours after infection, the cells were either treated with KIF or transfected with EDEM1 siRNA. Forty hours later, culture medium was replaced with 100 μg/ml cycloheximide (CHX). Cells, including floating cells, were harvested at different time points after CHX addition, and immunoblotting was performed to determine the amount of HCV E2.

Plasmid Transfection and Immunoprecipitation—HuH-7 or 293T cells were seeded in 6-well cell culture plates at 3×10^5 cells/well and cultured overnight. Plasmid DNA was transfected into cells using TranIT-LT1 transfection reagent (Mirus, Madison, WI). Cells were harvested at 48 h after transfection, washed once with 1 ml of PBS, and lysed in 200 μl of lysis buffer (20 mM Tris-HCl, pH 7.4, 135 mM NaCl, 1% Triton X-100, and 10% glycerol supplemented with 50 mM NaF, 5 mM Na_3VO_4, and protease inhibitor mixture tablets (Roche Diagnostics). Cell lysates were sonicated at 4 °C for 10 min, incubated for 30 min at 4 °C, and centrifuged at 14,000 × *g* for 5 min at 4 °C. After preclearing for 2 h, the supernatants were immunoprecipitated overnight by rotating with 1.5 μl of anti-HA monoclonal antibody (16B12) or anti-HCV E2 monoclonal antibody (clone 8D10-3) at 4 °C. The immunocomplexes were then captured on protein G-agarose beads (Invitrogen) by rotation-incubation at 4 °C for 3 h. Beads were subsequently precipitated by centrifugation at 800 × *g* for 1 min and washed five times with lysis buffer. Finally, proteins bound to the beads were boiled in 40 μl of SDS sample buffer and subjected to SDS-PAGE.

Western Blotting—Proteins resolved by SDS-PAGE were transferred onto PVDF membranes (Immobilon; Millipore). After blocking in 2% skim milk, the membranes were probed with primary antibodies followed by exposure to peroxidase-conjugated secondary antibodies and visualization with an ECL Plus Western blotting detection system (GE Healthcare). The intensity of the bands was measured using a computerized imaging system (ImageJ software; National Institutes of Health).

Small Interfering RNA (siRNA) Transfection—HuH-7 cells were transfected with duplex siRNAs at a final concentration of 10 nM using Lipofectamine RNAiMAX (Invitrogen). Three siRNAs for each gene were examined for knock-down efficiency and cytotoxic effects. The siRNA with best performance was selected for further experiments. Target sequences of the siRNAs which exhibited the best knock-down efficiencies were as follows: EDEM1 (sense) 5′-CAUAUCCUCGGGUGAAUCUtt-3′, EDEM2 (sense) 5′-GAAUGUCUCAGAAUUCCAAtt-3′, EDEM3 (sense) 5′-CAUGAGACUACAAAUCUUAtt-3′, IRE1 (sense) 5′-GGACGUGAGCGACAGAAUAtt-3′. 5′-GGUGUCCUUACCAUACUAAtt-3′ served as a negative control. The lowercase letters denote overhanging deoxyribonucleotides.

Quantification of HCV Core and RNA—HCV core was quantified using an enzyme immunoassay (Ortho HCV antigen ELISA kit; Ortho Clinical Diagnostics, Tokyo, Japan). HCV RNA was quantified as described (17).

Statistical Analysis—Student's *t* test was employed to calculate the statistical significance of the results. $p < 0.05$ was considered significant.

RESULTS

HCV Infection Induces XBP1 mRNA Splicing and EDEM Expression—XBP1 plays a key role in activating the ERAD pathway, which mediates unfolded protein response in the ER. Under conditions of ER stress, XBP1 mRNA is processed by unconventional splicing and translated into functional XBP1, which in turn mediates transcriptional up-regulation of a variety of ER stress-dependent genes. The resultant activation of downstream pathways boosts the efficiency of ERAD, which coincides with elevated transcription of EDEMs. To validate our method for detecting activation of the ERAD pathway, we exposed HuH-7.5.1 cells to TM, which is a typical ER stress inducer, and performed an assay to quantify spliced XBP1 mRNA, as described under "Experimental Procedures," at different time points after treatment. The spliced form of XBP1 mRNA started accumulating within these cells as early as 2 h after exposure to TM (Fig. 1*A*), and levels remained elevated until at least 12 h after treatment. Quantitative RT-PCR showed that mRNA levels of EDEM1, EDEM2, and EDEM3 were elevated in TM-treated cells whereas ER ManI, which is not an ER stress-responsive gene, did not show any up-regulation (Fig. 1*B*). To examine involvement of the ERAD pathway in the HCV life cycle, we infected HuH-7.5.1 cells with JFH-1 at m.o.i. of 5 and analyzed XBP1 mRNA splicing and EDEM up-regulation. Upon infection, the fragment corresponding to spliced XBP1 mRNA, was detectable 8 h after infection, and the difference in splicing between mock- and HCV-infected cells became more pronounced at 48 h after infection and then persisted (Fig. 1*C*). Increased levels of XBP1 mRNA splicing were dependent on the m.o.i. (supplemental Fig. 1*A*), suggesting that expression of active XBP1 was induced by HCV infection. A small amount of spliced XBP1 was detected in mock-infected cells, presumably because of some intrinsic stress. A 3.1-fold increase in the level of EDEM1 mRNA was observed at 3–4 days after infection ($p < 0.05$). Increases in EDEM2 and EDEM3 mRNA levels were moderate and reached ~1.5-fold, whereas ER ManI mRNA exhibited no change after infection (Fig. 1*D*). Expression of EDEMs, particularly EDEM1, was up-regulated in accordance with HCV infection titers (supplemental Fig. 1*B*). Knocking down the IRE1 gene (Fig. 1*E*) effectively reversed the accumulation of spliced XBP1, as well as the transcriptional up-regulation of EDEM1 (Fig. 1*F*), thus confirming that HCV infection induces ERAD through the IRE1-XBP1 pathway.

To enable a comprehensive investigation of the transcriptional changes that occur, up- and down-regulation of the transcriptome was examined in HCV-infected cells and in TM-treated cells. The results were compared with those of mock-transfected cells at each time point. A range of genes involved in ER stress was found to be regulated in HCV-infected and in TM-treated cells (Fig. 2*A*). EDEM1 was signifi-

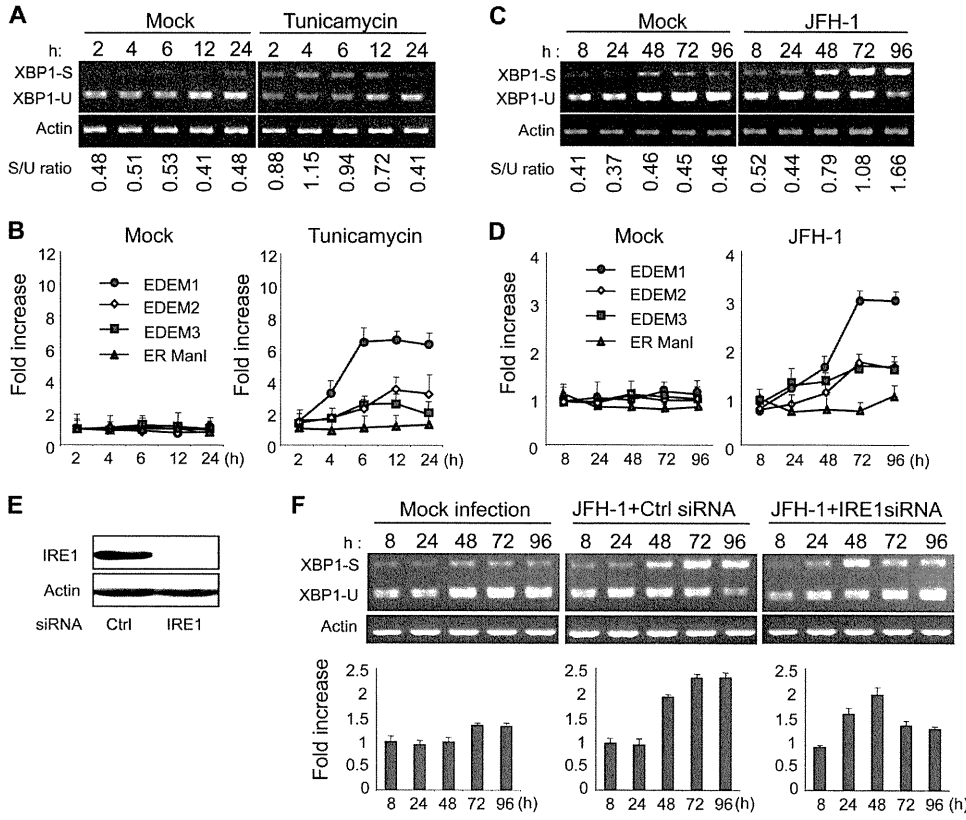

FIGURE 1. **Splicing of XBP1 mRNA and induction of ERAD gene expression in HCV JFH-1-infected cells.** *A*, splicing of XBP1 mRNA analyzed in mock- and TM (5 μg/ml)-treated HuH-7.5.1 cells at different time points after treatment. The *upper* and *lower bands* represent spliced and unspliced RNA, respectively. The *numbers* at the *bottom* of the *panel* indicate the density ratios of bands corresponding to spliced and unspliced XBP1. *B*, graphs showing the -fold induction of EDEM1, EDEM2, EDEM3, and ER Man1 mRNA in HuH-7.5.1 cells treated or untreated with TM. Data are normalized to GAPDH expression levels. The mean ± S.D. (*error bars*) of three independent experiments are shown. *C*, splicing of XBP1 mRNA analyzed in mock- and HCV JFH-1-infected HuH-7.5.1 cells (m.o.i. 5) at different time points after infection. *Numbers* at the *bottom* of the *panel* indicate the density ratios of bands corresponding to spliced and unspliced XBP1. *D*, real-time PCR analysis of EDEM1, EDEM2, EDEM3, and ER ManI mRNA induction in mock- and HCV-infected cells. Data are normalized to GAPDH expression. The mean ± S.D. of three independent experiments are shown. Note that a reduction in the level of GAPDH mRNA within infected cells was not observed until 96 h after infection when a slight decrease was observed. This led us to use GAPDH as a housekeeping gene in our experiments. *E*, Western blotting of IRE1 in cells transfected with mock or gene-specific siRNA of IRE1. *F*, splicing of XBP1 mRNA and induction of EDEM1 in HCV-infected cells after knocking down of the IRE1 gene. HuH-7.5.1 cells infected with JFH-1 at a m.o.i. of 5 were transfected with mock (*center*) or IRE1-specific siRNA (*right*) 48 h after infection, after which splicing of XBP1 (*upper*) and transcriptional up-regulation of EDEM1 (*lower*) were examined at the indicated time points after infection. The mean ± S.D. of two independent experiments are shown.

cantly up-regulated upon HCV infection, whereas expression levels of EDEM2 and EDEM3 remained unchanged. Although transcriptional changes caused by HCV infection in many of the genes listed are analogous to those that occur in cells treated with TM, up-regulation of two ER chaperone proteins, GRP78 and GRP94, was induced by TM treatment but not by HCV infection. This differential induction was confirmed by a reporter assay for GRP78 promoter and GRP94 promoter activities (Fig. 2*B*). These results are in agreement with a previously described finding that GRP78 and GRP94 are not responsive to HCV infection in hepatoma cells (18). It remains likely that HCV infection interferes with transcriptional activation of some ER chaperone proteins; however, the mechanism by which this occurs remains to be elucidated.

EDEMs Cause Ubiquitylation of HCV Glycoproteins and Enhance Their Degradation—Because EDEMs have been reported to enhance proteasomal degradation of ERAD substrates through direct binding, we investigated the interaction of EDEMs with HCV glycoproteins in 293T cells by co-transfecting the expression plasmids for E1dTM or E2dTM together with plasmids carrying either EDEM or ER ManI genes. Immunoprecipitation and immunoblotting demonstrated that each EDEM, but not ER ManI, was capable of interacting with E2 (Fig. 3*A*) and E1 (supplemental Fig. S2). HCV glycoproteins displayed enhanced mobility when co-expressed with EDEM1, EDEM3, or ER ManI, which could be due to the mannosidase activity of these proteins, which is lacking in EDEM2 (6). HCV primarily replicates in hepatocytes so we examined the interaction of EDEMs with E2dTM in HuH-7 cells as well, which yielded similar results (data not shown). E2dTM lacks the transmembrane domain, which could affect its folding and ER retention and thus modulate the ability of this protein to interact with EDEMs and ER ManI. Second, E1 and E2 glycoproteins assemble as noncovalent heterodimers to make functional complexes, which may alter the interaction of these proteins with EDEMs. To address these issues, we co-transfected HuH-7 cells with plasmids carrying full-length E1E2 glycoproteins together with plasmids carrying either EDEMs or ER ManI. Similar phenotypes were produced following transfection full-length E1E2 proteins (supplemental Fig. S3*A*), demonstrating that functional complexes of HCV glycoproteins bind with EDEMs. Recently, we have reported on the development of a

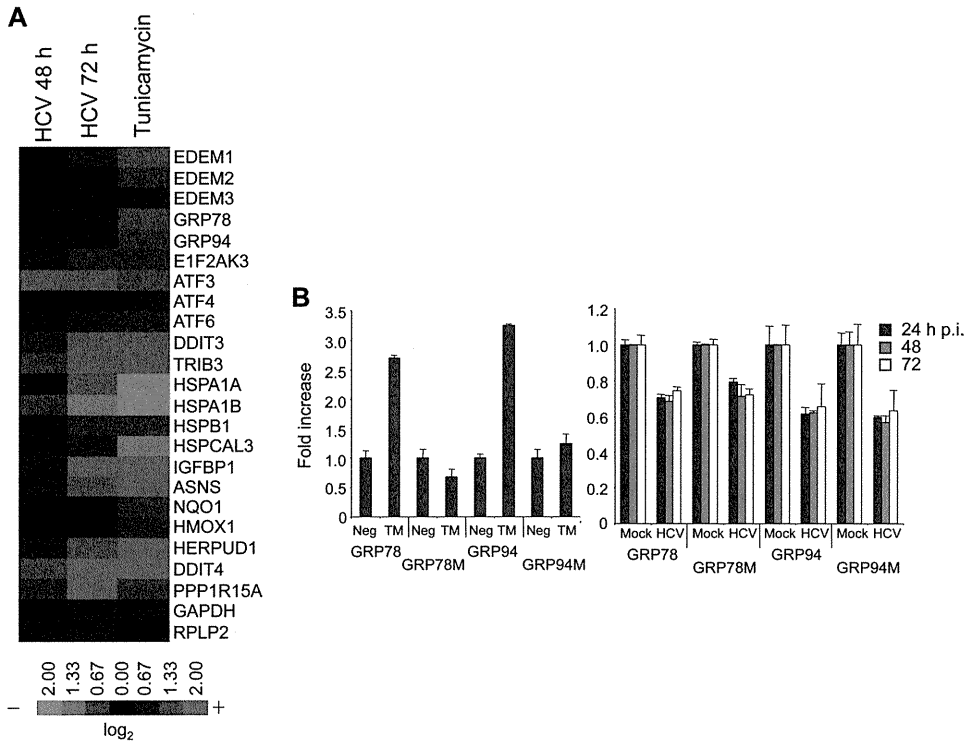

FIGURE 2. **Comprehensive analysis of ERAD gene expression in JFH-1-infected HuH-7.5.1 cells.** *A*, HuH-7.5.1 cells treated with TM (5 μg/ml) for 12 h or infected with JFH-1 for 48 and 72 h were subjected to microarray analysis, along with their negative controls. Expression of ER stress genes is shown as a heat map. *Red* and *green* indicate up- and down-regulation, respectively. Information on each gene shown is indicated on the 3D-Gene web site. *B*, GRP78 and GRP94 induction in TM-treated (*left*) and HCV-infected cells (*right*). GRP78M and GRP94M represent the defective promoters. The mean ± S.D. (*error bars*) of three independent experiments are shown.

packaging system of HCV subgenomic replicon sequences through the provision of viral core NS2 proteins in *trans* (19). Transcomplementation with core NS2 proteins resulted in successful packaging of the viral sequences; therefore, plasmids carrying these proteins are a valid construct by which to examine the interaction of envelope proteins with ERAD machinery. Thus, we performed an immunoprecipitation assay of HuH-7 cells co-transfected with core NS2 and EDEMs. In agreement with our previous results, EDEMs, but not ER ManI, were observed to bind to HCV E2 protein (supplemental Fig. S3*B*). To examine the functional importance of this interaction, we analyzed the ubiquitylation of HCV E2 protein in cells co-transfected with HCV E2 and EDEM proteins. An immunoprecipitation assay revealed that overexpression of EDEM1 and EDEM3, but not of EDEM2 and ER ManI, dramatically increased the ubiquitylation of HCV glycoprotein (Fig. 3*B*). In mammals, the ER membrane ubiquitin-ligase complex involved in the dislocation of ERAD substrates, and their ubiquitylation contains the ER membrane adaptor SEL1L. It has recently been shown that SEL1L interacts with EDEM1 in cells and functions as a cargo receptor for ERAD substrates (20); however, it is unknown whether SEL1L interacts with other EDEMs. We therefore assessed whether SEL1L interacts with EDEM1, EDEM2, EDEM3, and ER ManI in cells (Fig. 3*C*). Interestingly, endogenous SEL1L co-precipitated with EDEM1 and EDEM3, whereas little to no interaction was observed with EDEM2 and ER ManI. Collectively, it is likely that, although all EDEMs can recognize HCV E1 and E2, EDEM1 and EDEM3 are involved in the ubiquitylation of HCV glycoproteins by delivering them to SEL1L-containing ubiquitin-ligase complexes. To investigate further the role of EDEMs in quality control of HCV glycoproteins, we measured the steady-state level of HCV E2 protein after EDEM knockdown. Transfection of HCV-infected cells with siRNAs against EDEM1, EDEM2, or EDEM3 caused a 60–80% reduction in mRNA levels of the respective genes (Fig. 3*D*) with no cytotoxic effects observed (data not shown). Immunoblotting showed a considerable increase in the steady-state level of viral E2 in EDEM1 siRNA-treated cells (Fig. 3*D*). We subsequently examined the turnover of E2 in cells with and without EDEM1 knockdown. In CHX half-life experiments, E2 protein was moderately unstable in control-infected cells, presumably via proteasomal degradation (Fig. 3*E*). Treatment with MG132, a proteasome inhibitor, blocked its destabilization (data not shown). In contrast, E2 was completely stable in EDEM1-knockdown cells during the chase period of time tested (Fig. 3*E*). Together, these results strongly suggest that EDEM1 and EDEM3, particularly EDEM1, are involved in the post-translational control of HCV glycoproteins.

Involvement of EDEM1 in the Production of Infectious HCV—Given the involvement of EDEMs in the turnover of HCV glycoproteins, we investigated whether EDEMs affect the replication and production of infectious virus particles. EDEMs were knocked down in HCV-infected HuH-7 cells by siRNA transfection, and the production of infectious particles was then monitored by measuring the extracellular infectivity titer. Knocking down of EDEM1 and EDEM3 in the infected cells resulted in ~3.1-fold ($p < 0.05$) and ~2.3-fold increases in virus production, respectively, compared with control cells. No effect

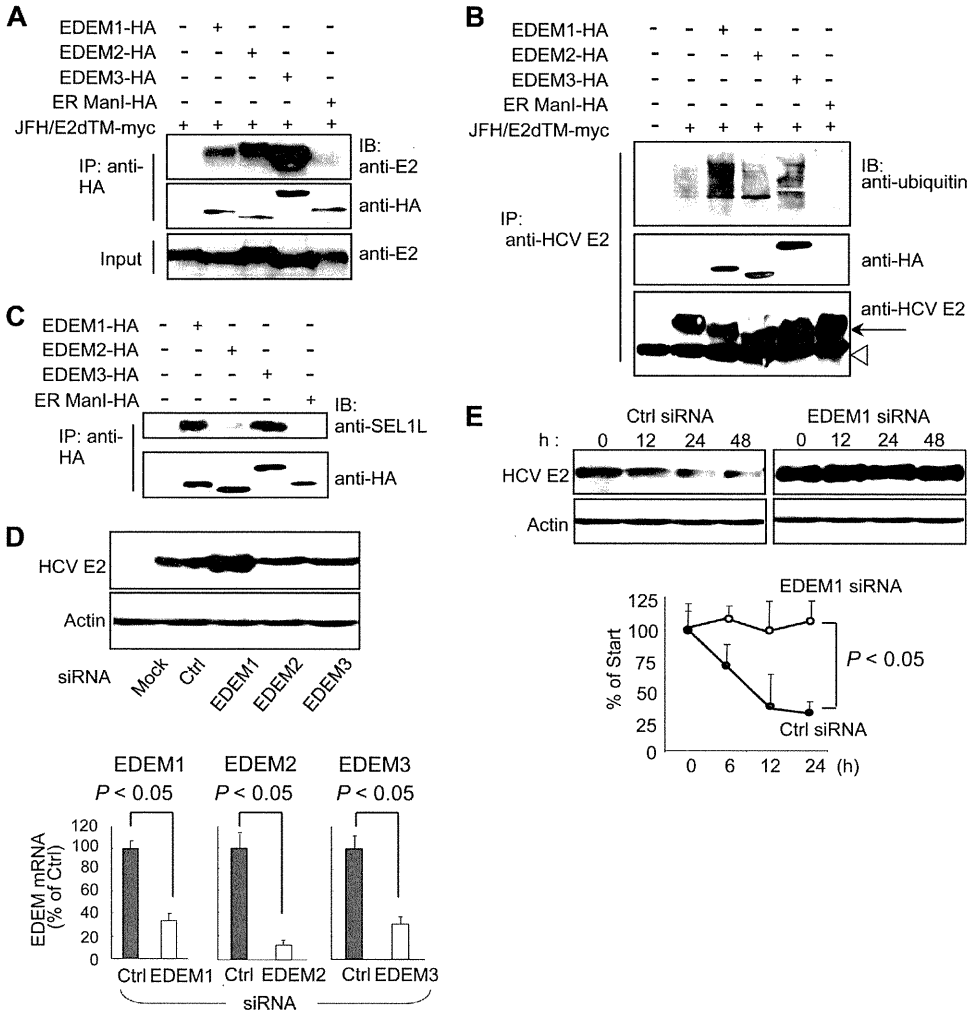

FIGURE 3. **EDEMs are involved in the degradation of HCV glycoproteins.** *A*, binding of EDEMs and ER ManI with HCV E2. 293T cells were seeded in 6-well plates at a density of 3×10^5 cells/well. After overnight incubation, cells were co-transfected with plasmids carrying HCV E2-myc (1 μg) and EDEM1-HA, EDEM2-HA, EDEM3-HA, or ER ManI-HA proteins (1 μg each). Forty-eight hours later, cells were harvested, immunoprecipitated (*IP*) with anti-HA antibodies, and Western blotting (*IB*) was performed with the indicated antibodies. *B*, ubiquitylation of HCV E2 protein in cells co-transfected with HCV E2 and EDEM plasmids. 293T cells were seeded in 6-well plates at a density of 3×10^5 cells/well. Twenty-four hours later, the cells were co-transfected with plasmids carrying HCV E2-myc (1 μg) and EDEM1-HA, EDEM2-HA, EDEM3-HA, or ER ManI-HA genes (1 μg each). Forty-eight hours later, the cells were harvested and immunoprecipitated with anti-E2 antibodies, and Western blotting was performed with the indicated antibodies. *Arrow*, HCV E2; *open arrowhead*, immunoglobulin heavy chain. *C*, binding of EDEMs and ER ManI with endogenous SEL1L in cells. *D*, steady-state level of HCV E2 in HCV-infected HuH-7 cells after EDEM knockdown (*upper*). The knockdown efficiencies of the respective siRNAs are shown in the *lower panel*. Values are normalized to GAPDH expression levels, and normalized values in negative control cells have been arbitrarily set at 100%. *E*, stability of HCV E2 protein in EDEM1 knockdown cells. HCV-infected HuH-7 cells were transfected with control or EDEM1 siRNA. Forty hours later, the cells were exposed to CHX (100 μg/ml) for 0, 12, 24, and 48 h, followed by immunoblotting. Specific signals were quantified by densitometry, and the percent of HCV E2 remaining was compared with initial levels. The mean ± S.D. (*error bars*) of two independent experiments are shown.

on virus production was observed following EDEM2 gene silencing (Fig. 4*A*). On the other hand, no significant differences were observed with regard to intracellular HCV core protein levels among mock- and EDEM siRNA-transfected cells (Fig. 4*B*), which indicates that replication of the viral genome is not affected by EDEM proteins. To examine further whether this effect on virus production was due to turnover of HCV envelope proteins, we performed loss-of-EDEM-function experiments in HuH-7 cells carrying HCV subgenomic replicons. Because the replicons do not require envelope proteins, they should be insensitive to the expression levels of genes involved in the ERAD pathway. As expected, siRNA-mediated knockdown of EDEMs resulted in little to no change in genome replication (supplemental Fig. S4*A*). To investigate further the participation of EDEMs in the HCV life cycle, HCV-infected cells were examined 48 h after transfection with an expression plasmid for either EDEM1, EDEM2, or EDEM3. As expected, exogenous expression of EDEM1 in the infected cells led to a 2.4-fold decrease in virus production compared with mock-transfected cells ($p < 0.05$) (Fig. 4*C*). A moderate decrease of 1.7-fold was observed in the cells overexpressing EDEM3 protein. Ectopic expression of EDEMs and ER ManI did not cause any change in intracellular HCV core protein levels (Fig. 4*D*). Similarly, little or no change was observed in genome replication when plasmids carrying EDEMs were introduced into HCV subgenomic replicon cells (supplemental Fig. S4*B*). These results indicate that EDEM1 and EDEM3, particularly EDEM1, regulate virus production, possibly through post-translational control of HCV glycoproteins.

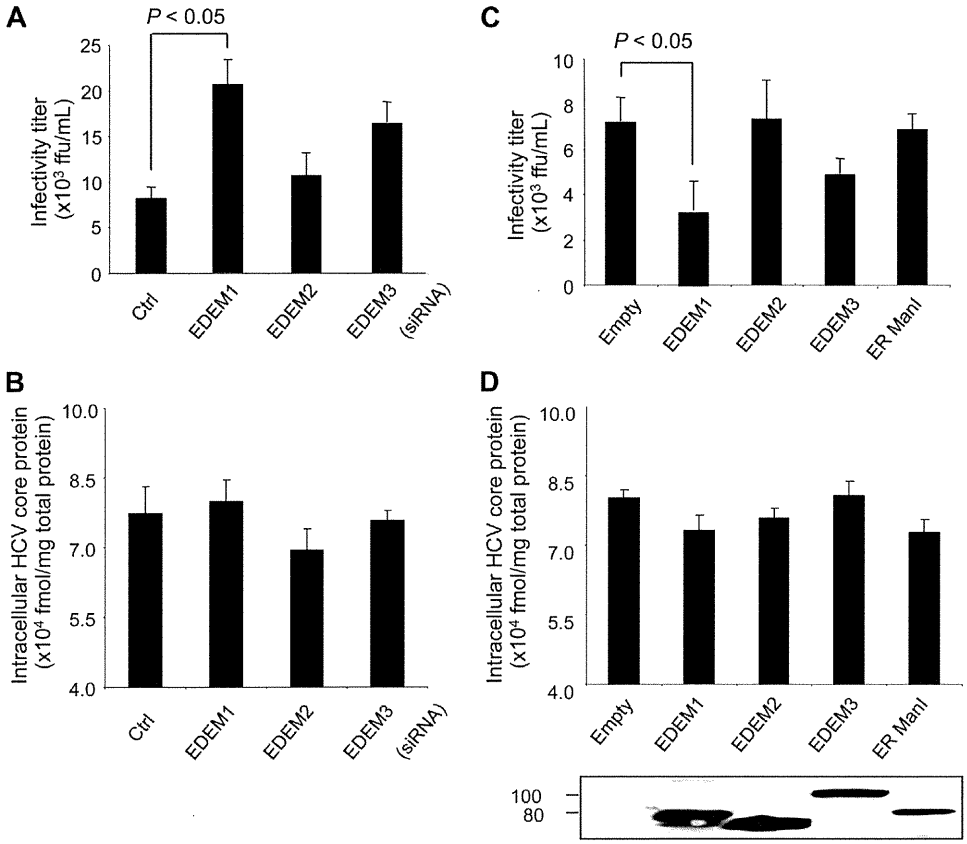

FIGURE 4. **Role of EDEMs in HCV replication and production of infectious virus particles.** *A*, HCV production in HuH-7 cells transfected with EDEM siRNAs. Cells were infected with JFH-1 at a m.o.i. of 1. Twenty-four hours later, the cells were transfected with the indicated siRNAs at a final concentration of 10 nM. The culture medium was harvested 48 h later and was used to infect naïve HuH-7.5.1 cells seeded in a 96-well plate. Immunostaining using anti-HCV core antibodies was performed at 72 h after infection, and focus-forming units were counted. *B*, siRNA-transfected and HCV-infected cells described in *A* harvested at 48 h after infection. Intracellular HCV core protein was measured. The values were normalized to total protein in the cell lysate samples. *C*, HCV production in HuH-7 cells transfected with plasmids carrying EDEM1-HA, EDEM2-HA, EDEM3-HA, or ER ManI-HA genes. *D*, intracellular HCV core protein within the cells described in *C*. Expression levels of the EDEMs and ER ManI were determined by anti-HA immunoblotting. The mean ± S.D. (*error bars*) of three independent experiments are shown in all of the *panels*.

Chemical Inhibition of the ERAD Pathway Increases HCV Production—KIF, a potent inhibitor of ER mannosidase, is reported to inhibit the ERAD pathway. When HCV-infected cells were treated with KIF, virus production increased in the culture medium in a dose-dependent manner (Fig. 5*A*, *left*), and the steady-state level of E2 in the cells increased accordingly (Fig. 5*A*, *right*). No change was observed in intracellular HCV core protein levels after KIF treatment (Fig. 5*A*, *center*). Kinetic analyses showed that E2 was stabilized dramatically in KIF-treated cells (Fig. 5*B*), whereas the fate of HCV core protein, a nonglycoprotein, was not affected by KIF treatment (supplemental Fig. S5). No effect on virus replication was observed when the cells harboring JFH-1 subgenomic replicons were treated with KIF (data not shown).

On the basis of these findings, one may hypothesize that KIF contributes to the stabilization of HCV glycoprotein(s) by interfering with the interaction between (i) EDEMs and viral proteins, or (ii) EDEMs and SEL1L. To address this, HCV E2 was co-expressed in 293T cells with EDEM1, EDEM2, EDEM3, or ER ManI in the presence or absence of KIF, followed by immunoprecipitation (Fig. 5*C*). E2 was shown to interact with EDEM1, EDEM2, and EDEM3, analogous to the data shown in Fig. 3*A*, and KIF did not block the interactions. Decreased electrophoretic mobility of E2 was detected in KIF-treated cells, possibly due to a change in glycan composition caused by inhibition of mannosidase activity. These findings led us to investigate whether the glycans on HCV glycoproteins are required for binding to EDEMs. We generated E1 and E2 mutants by replacing their *N*-glycosylation sites with glutamine residues and analyzed their interaction with EDEMs. Removal of the glycans did not inhibit the binding of E1 and E2 proteins to EDEM, demonstrating that *N*-glycans on the surface of viral proteins are not indispensible for an interaction between EDEMs and HCV glycoproteins to occur (supplemental Fig. S6). The effect of KIF on the association of EDEMs with downstream ERAD machinery was examined further. In cells co-expressing E2 and EDEMs, the interaction of SEL1L with EDEM1 and EDEM3 was significantly reduced in the presence of KIF ($p < 0.05$) (Fig. 5*C*). Consistent with these results, KIF abrogated the EDEM1- and EDEM3-mediated ubiquitylation of HCV E2 protein (Fig. 5*D*). This inhibitory effect of KIF on the SEL1L-EDEM interaction was also observed in HuH-7 cells (supplemental Fig. S7). These results suggest that KIF stabilizes HCV glycoproteins by interfering with the SEL1L-EDEM interaction and thus leads to an increase in virus production.

Role of ERAD in the Life Cycle of JEV—This study demonstrates involvement of the ERAD pathway in HCV production. However, the role of this pathway in the production of other

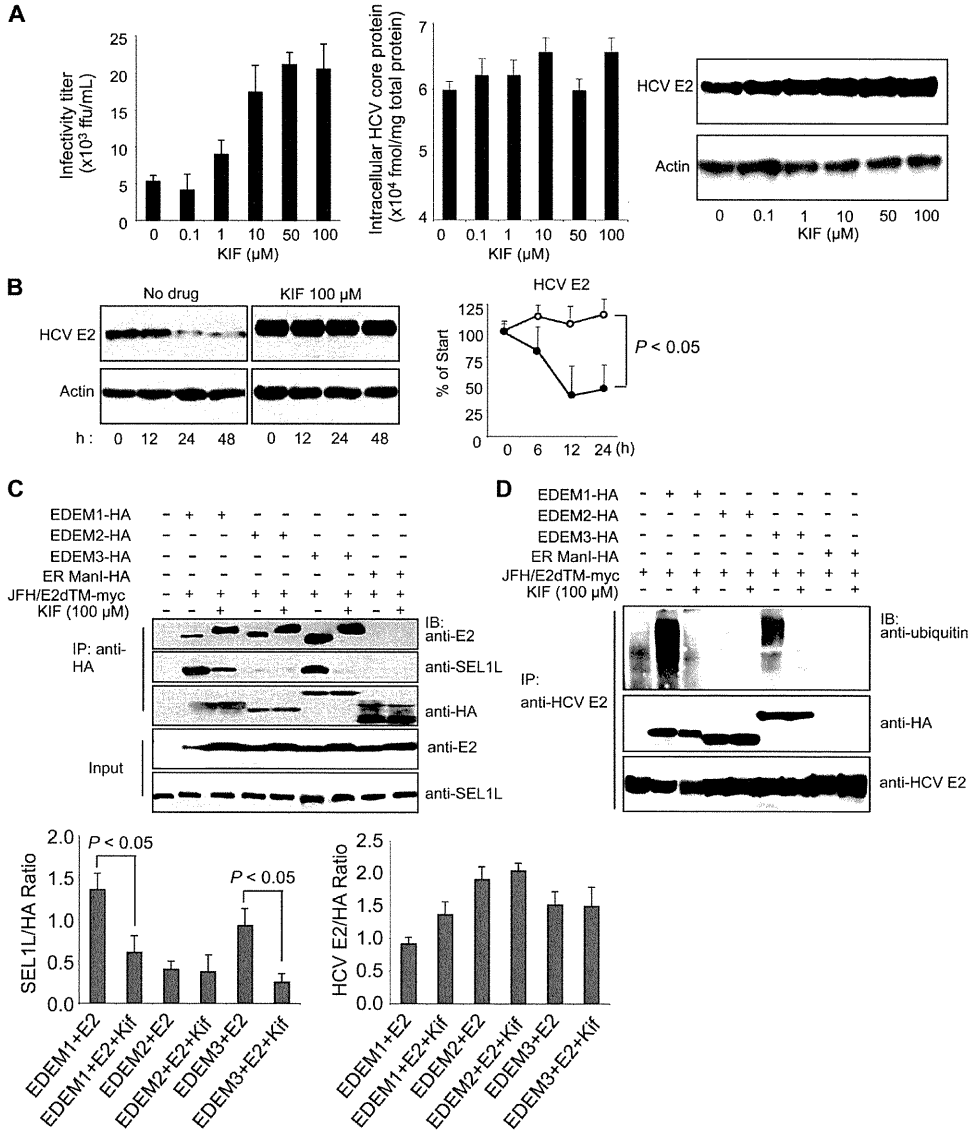

FIGURE 5. **Effect of KIF on HCV production and stability of E2.** *A*, extracellular HCV titer, intracellular HCV core protein expression, and steady-state level of HCV E2 in HuH-7 cells treated with different concentrations of KIF. *B*, CHX-based HCV protein stability assay of HCV E2 protein in KIF-treated cells as described in Fig. 3*E*. E2 protein levels normalized to actin levels are shown in the *graph* on the *right*. The *open* and *filled circles* indicate KIF-treated and nontreated cells, respectively. The mean ± S.D. (*error bars*) of two independent experiments are shown. *C*, binding of EDEMs and ER ManI with HCV E2 and SEL1L in 293T cells in the absence or presence of KIF. 293T cells were seeded in 6-well plates at a density of 3×10^5 cells/well. After overnight incubation, the cells were co-transfected with plasmids carrying HCV E2-myc (1 μg) and EDEM1-HA, EDEM2-HA, EDEM3-HA, or ER ManI-HA proteins (1 μg each). After 6 h, the culture medium was replaced with fresh or KIF-containing medium (100 μM). Forty-eight hours later, the cells were harvested and immunoprecipitated (*IP*) with anti-HA antibodies, after which Western blotting (*IB*) was performed with the indicated antibodies. Specific signals were quantified by densitometry, and the ratio between HCV E2 and HA (*right graph*) and between SEL1L and HA (*left graph*) in the same *lanes* is plotted on the graphs. The mean ± S.D. of three independent experiments are shown. *D*, EDEM protein-mediated ubiquitylation of HCV E2 protein in 293T cells in the absence or presence of KIF. The experimental procedure was the same as that described in Fig. 5*C*, except that immunoprecipitation was performed with anti-HCV E2 antibodies.

viruses is still unknown. To this end, we examined its role in the life cycle of JEV, another member of the Flaviviridae family. In contrast to HCV, KIF treatment had little effect on JEV production in infected cells (Fig. 6*A*) or the steady-state level of viral E glycoprotein (Fig. 6*B*). Interaction of EDEMs with JEV E was analyzed further. Neither EDEMs nor ER ManI was found to interact with JEV E in cells (Fig. 6*C*), indicating no significant role of the ERAD pathway in the JEV life cycle. Altogether, these results strongly suggest that the ERAD pathway is involved in the quality control of glycoproteins of specific viruses, possible through an interaction with EDEM(s), and subsequent regulation of virus production.

DISCUSSION

Accumulating evidence points to a role of the ERAD pathway in the pathogenesis of different genetic and degenerative diseases. However, the involvement of ERAD in the life cycle of viruses and infectious diseases remains poorly understood. Until recently, an experimental HCV cell culture infection system has been lacking such that studies evaluating the effect of HCV infection on the ERAD pathway were performed by either using HCV subgenomic replicons which lack structural proteins or by ectopic expression of one or multiple structural proteins (21, 22). However, this problem was solved by identifica-

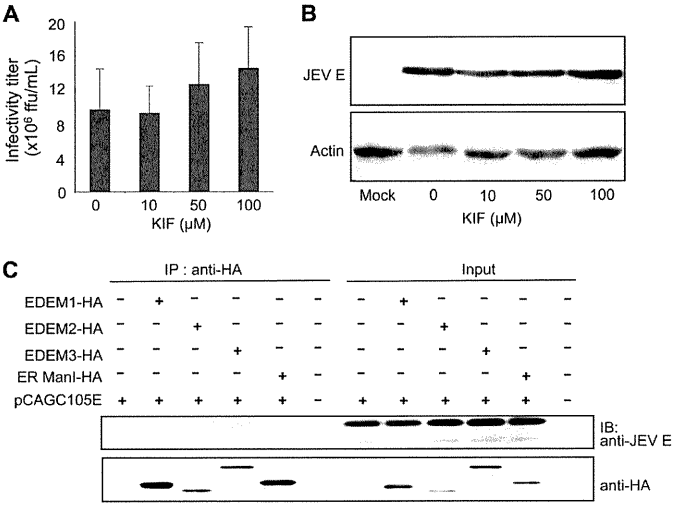

FIGURE 6. **Binding of JEV envelope glycoprotein with EDEMs and effect of KIF on JEV production.** *A*, JEV production in HuH-7 cells treated with KIF. The mean ± S.D. (*error bars*) of three independent experiments are shown. *B*, effect of KIF on the steady-state level of JEV envelope protein. *C*, binding of EDEMs with the JEV envelope.

tion of an HCV clone, JFH-1, capable of replicating and assembling infectious virus particles in cultured hepatocytes (15). In the present study, we used JFH-1 to examine the effect of HCV infection on activation of the ERAD pathway and its role in the virus life cycle. Our results show that the ERAD pathway is activated in HCV-infected cells, as evidenced by the maturation of XBP1 mRNA to its active form and up-regulation of EDEM1 (Fig. 1, *A–D*). Knocking down IRE1 reversed the induction of EDEM1, indicating that HCV infection-induced activation of the ERAD pathway is mediated through IRE1 (Fig. 1*F*). Loss- and gain-of-function analyses indicated that EDEM1 and EDEM3, particularly EDEM1, are involved in the post-translational control of HCV glycoproteins by which viral production is down-regulated (Figs. 3, *D* and *E*, and 4*A*). Our results suggest that EDEM1 and EDEM3 play a role in delivery of viral glycoproteins to the SEL1L-containing ubiquitin-ligase complex. It has recently been reported that coronavirus infection causes an accumulation of EDEM1 in membrane vesicles which are sites of viral replication, but that EDEM1 is not required for coronavirus replication (23). To our knowledge, the present study is the first to demonstrate regulation of the viral life cycle by ERAD machinery through interaction of EDEMs with viral glycoproteins.

We propose that the mechanisms described here are important during the early stages of establishing persistent HCV infection. ER stress caused by high levels of HCV infection during the acute phase presumably results in activation of the ERAD pathway. Induced EDEMs enhance the degradation of HCV envelope proteins, thereby reducing virus production. Maintenance of moderately low levels of HCV in the infected liver may contribute to the persistence of HCV infection, often associated with a lengthy asymptomatic phase that can last for decades. A range of viruses, including flaviviruses such as JEV, dengue virus, and West Nile virus, have been reported to induce XBP1 mRNA splicing triggered by ER stress (2, 3, 24). However, we demonstrate here that, in contrast to HCV, the envelope protein of JEV, which causes acute encephalitis, is not recognized by EDEMs, and the ERAD pathway does not control JEV production.

N-Linked glycoproteins displaying the glycan precursor Glc1Man9GlcNAc2 bind ER chaperones, such as calnexin or calreticulin, which facilitates protein folding. Removal of the terminal Glc from glycans disrupts this interaction with chaperones leading to Man trimming and delivery to ERAD machinery. A glucosyltransferase can transfer the terminal Man-linked Glc back to glycans, thereby allowing the "calnexin cycle" to continue until the glycoproteins are properly folded (for review, see Ref. 25). During this cycle, the decision of when to abandon additional folding attempts for immature polypeptides and to direct them instead toward the degradation pathway appears to be a crucial element of protein quality control. The basis by which this occurs, however, is not fully understood. Here, we demonstrate that stabilization of HCV envelope proteins and increased virus production occurs with KIF treatment (Fig. 5, *A* and *B*) and with gene silencing of either EDEM1 or EDEM3 (Figs. 3, *D* and *E*, and 4*A*). It is generally accepted that ERAD functions to eliminate proteins that are unable to adopt their native structure after translocation into the ER. From our results, however, one could argue that, during the HCV life cycle, at least a fraction of the competently folded viral glycoprotein intermediates may be released from the calnexin cycle before maturation and thereby be recognized as ERAD substrates. As suggested previously, the processes of protein folding and ERAD compete to some extent for newly synthesized polypeptides (26, 27). Under conditions in which high concentrations of ERAD-related factors are found in the ER due to induction of ER stress by viral infection, activated ERAD machinery may efficiently capture protein intermediates with folding/refolding capacity and cause premature termination of chaperone-assisted protein folding.

EDEM1 has recently been found to bind SEL1L, which is involved in the translocation of ERAD substrates from the ER to the cytoplasm (20). Our results demonstrate efficient binding of EDEM1 and EDEM3 to SEL1L, whereas EDEM2 exhibits only residual binding. In agreement with these results, increased ubiquitylation of HCV E2 protein was observed in cells overexpressing EDEM1 and EDEM3, but not in cells overexpressing the EDEM2 ortholog (Fig. 3*B*). Furthermore, KIF inhibited the binding of EDEM1 and EDEM3 with SEL1L, thus abrogating the ubiquitylation and enhancing the stability of HCV E2 protein (Fig. 5, *B* and *D*). It has been reported that KIF inhibits the interaction between EDEM1 and SEL1L, thus stabilizing ERAD substrates (4). Therefore, our results confirm previous findings and show that, along with EDEM1, KIF inhibits the binding of SEL1L to EDEM3. Furthermore, we have been the first to show that HCV E2 is a virus-derived ERAD substrate that can be used to analyze the mechanisms of this pathway. Taken together, our results indicate that EDEM1 and EDEM3, but not EDEM2, might be involved in targeting ERAD substrates to the translocation machinery, which may partly explain the different roles of the three EDEMs in HCV production. Although both EDEM1 and EDEM3 bind SEL1L and HCV envelope proteins, EDEM1 appears to have a larger role in regulation of HCV production than EDEM3. This is supported further by the finding that enhanced ubiquitylation of HCV E2 occurs in the presence

of EDEM1 overexpression (Figs. 3*B* and 5*D*). In EDEM3-knockdown cells, EDEM1 may take over the function of delivering ERAD substrates to the translocation machinery. We also speculate that EDEM1 may function as a helper for EDEM3. This is supported by the observation that EDEM1 and EDEM3 synergistically increase HCV production when knocked down together (data not shown). HCV glycoproteins are a suitable means by which to investigate differences and redundancies pertaining to the role of EDEMs in the ERAD pathway.

HCV-infected and TM-treated cells demonstrated the greatest activation of EDEM1 transcript production among EDEMs (Fig. 1, *C* and *D*, and supplemental Fig. S1). Although it is known that XBP1 binds to specific ER stress-responsive *cis*-acting elements to induce EDEMs (28, 29), the exact mechanism of transcriptional regulation is not fully understood. It will be interesting to examine regulatory mechanism(s) specific to individual EDEM homologs in an ER stress-dependent or -independent manner.

These findings highlight the crucial role of the ERAD pathway in the HCV life cycle. Further studies are needed to clarify the details of this complex pathway. The data generated in this work, however, further contribute to our understanding of the mechanisms that govern the maturation and fate of viral glycoproteins in the ER.

Acknowledgments—We thank Dr. F. V. Chisari for the HuH-7.5.1 cells, Drs. N. Hosokawa and K. Nagata for the EDEM expression plasmids, Dr. K. Mori for the reporter plasmids of GRP78 and GRP94, and Drs. C. K. Lim and T. Takasaki for the anti-JEV antibody. We thank Drs. Chia-Yi Yu and Yi-Ling Lin for valuable advice and T. Date, M. Kaga, M. Sasaki, and T. Mizoguchi for assistance.

REFERENCES

1. Vembar, S. S., and Brodsky, J. L. (2008) *Nat. Rev. Mol. Cell Biol.* **9,** 944–957
2. Yu, C. Y., Hsu, Y. W., Liao, C. L., and Lin, Y. L. (2006) *J. Virol.* **80,** 11868–11880
3. Barry, G., Fragkoudis, R., Ferguson, M. C., Lulla, A., Merits, A., Kohl, A., and Fazakerley, J. K. (2010) *J. Virol.* **84,** 7369–7377
4. Isler, J. A., Skalet, A. H., and Alwine, J. C. (2005) *J. Virol.* **79,** 6890–6899
5. Helenius, A., and Aebi, M. (2004) *Annu. Rev. Biochem.* **73,** 1019–1049
6. Mast, S. W., Diekman, K., Karaveg, K., Davis, A., Sifers, R. N., and Moremen, K. W. (2005) *Glycobiology* **15,** 421–436
7. Hirao, K., Natsuka, Y., Tamura, T., Wada, I., Morito, D., Natsuka, S., Romero, P., Sleno, B., Tremblay, L. O., Herscovics, A., Nagata, K., and Hosokawa, N. (2006) *J. Biol. Chem.* **281,** 9650–9658
8. Bartenschlager, R., and Lohmann, V. (2000) *J. Gen. Virol.* **81,** 1631–1648
9. Reed, K. E., and Rice, C. M. (2000) *Curr. Top. Microbiol. Immunol.* **242,** 55–84
10. Zhong, J., Gastaminza, P., Cheng, G., Kapadia, S., Kato, T., Burton, D. R., Wieland, S. F., Uprichard, S. L., Wakita, T., and Chisari, F. V. (2005) *Proc. Natl. Acad. Sci. U.S.A.* **102,** 9294–9299
11. Zhao, Z., Date, T., Li, Y., Kato, T., Miyamoto, M., Yasui, K., and Wakita, T. (2005) *J. Gen. Virol.* **86,** 2209–2220
12. Tani, H., Shiokawa, M., Kaname, Y., Kambara, H., Mori, Y., Abe, T., Moriishi, K., and Matsuura, Y. (2010) *J. Virol.* **84,** 2798–2807
13. Yoshida, H., Haze, K., Yanagi, H., Yura, T., and Mori, K. (1998) *J. Biol. Chem.* **273,** 33741–33749
14. Murakami, K., Kimura, T., Osaki, M., Ishii, K., Miyamura, T., Suzuki, T., Wakita, T., and Shoji, I. (2008) *J. Gen. Virol.* **89,** 1587–1592
15. Wakita, T., Pietschmann, T., Kato, T., Date, T., Miyamoto, M., Zhao, Z., Murthy, K., Habermann, A., Kräusslich, H. G., Mizokami, M., Bartenschlager, R., and Liang, T. J. (2005) *Nat. Med.* **11,** 791–796
16. Lim, C. K., Takasaki, T., Kotaki, A., and Kurane, I. (2008) *Virology* **374,** 60–70
17. Takeuchi, T., Katsume, A., Tanaka, T., Abe, A., Inoue, K., Tsukiyama-Kohara, K., Kawaguchi, R., Tanaka, S., and Kohara, M. (1999) *Gastroenterology* **116,** 636–642
18. Deng, L., Adachi, T., Kitayama, K., Bungyoku, Y., Kitazawa, S., Ishido, S., Shoji, I., and Hotta, H. (2008) *J. Virol.* ***82,*** *10375–10385*
19. Masaki, T., Suzuki, R., Saeed, M., Mori, K., Matsuda, M., Aizaki, H., Ishii, K., Maki, N., Miyamura, T., Matsuura, Y., Wakita, T., and Suzuki, T. (2010) *J. Virol.* ***84,*** *5824–5835*
20. Cormier, J. H., Tamura, T., Sunryd, J. C., and Hebert, D. N. (2009) *Mol. Cell* **34,** 627–633
21. Tardif, K. D., Mori, K., Kaufman, R. J., and Siddiqui, A. (2004) *J. Biol. Chem.* **279,** 17158–17164
22. Chan, S. W., and Egan, P. A. (2005) *FASEB J.* **19,** 1510–1512
23. Reggiori, F., Monastyrska, I., Verheije, M. H., Calì, T., Ulasli, M., Bianchi, S., Bernasconi, R., de Haan, C. A., and Molinari, M. (2010) *Cell Host Microbe* **7,** 500–508
24. Medigeshi, G. R., Lancaster, A. M., Hirsch, A. J., Briese, T., Lipkin, W. I., Defilippis, V., Früh, K., Mason, P. W., Nikolich-Zugich, J., and Nelson, J. A. (2007) *J. Virol.* **81,** 10849–10860
25. Molinari, M. (2007) *Nat. Chem. Biol.* **3,** 313–320
26. Eriksson, K. K., Vago, R., Calanca, V., Galli, C., Paganetti, P., and Molinari, M. (2004) *J. Biol. Chem.* **279,** 44600–44605
27. Wu, Y., Swulius, M. T., Moremen, K. W., and Sifers, R. N. (2003) *Proc. Natl. Acad. Sci. U.S.A.* **100,** 8229–8234
28. Olivari, S., Galli, C., Alanen, H., Ruddock, L., and Molinari, M. (2005) *J. Biol. Chem.* **280,** 2424–2428
29. Yoshida, H., Matsui, T., Hosokawa, N., Kaufman, R. J., Nagata, K., and Mori, K. (2003) *Dev. Cell* **4,** 265–271

Biochemical and Biophysical Research Communications 410 (2011) 404–409

Contents lists available at ScienceDirect

Biochemical and Biophysical Research Communications

journal homepage: www.elsevier.com/locate/ybbrc

Development of recombinant hepatitis C virus with NS5A from strains of genotypes 1 and 2

Yuka Okamoto [a,b], Takahiro Masaki [a], Asako Murayama [a], Tsubasa Munakata [c], Akio Nomoto [d], Shingo Nakamoto [e], Osamu Yokosuka [e], Haruo Watanabe [b,f], Takaji Wakita [a], Takanobu Kato [a,*]

[a] Department of Virology II, National Institute of Infectious Diseases, Shinjuku-ku, Tokyo 162-8640, Japan
[b] Department of Pathology, Immunology, and Microbiology, Graduate School of Medicine, The University of Tokyo, Bunkyo-ku, Tokyo 113-0033, Japan
[c] The Tokyo Metropolitan Institute of Medical Science, Setagaya-ku, Tokyo 156-8506, Japan
[d] Institute of Microbial Chemistry, Shinagawa-ku, Tokyo 141-0021, Japan
[e] Department of Medicine and Clinical Oncology, Graduate School of Medicine, Chiba University, Chiba 260-0856, Japan
[f] National Institute of Infectious Diseases, Shinjuku-ku, Tokyo 162-8640, Japan

ARTICLE INFO

Article history:
Received 26 May 2011
Available online 6 June 2011

Keywords:
HCV
NS5A inhibitor
Virus assembly
JFH-1

ABSTRACT

Nonstructural protein 5A (NS5A) of hepatitis C virus (HCV) plays multiple and diverse roles in the viral lifecycle, and is currently recognized as a novel target for anti-viral therapy. To establish an HCV cell culture system with NS5A of various strains, recombinant viruses were generated by replacing NS5A of strain JFH-1 with those of strains of genotypes 1 (H77; 1a and Con1; 1b) and 2 (J6CF; 2a and MA; 2b). All these recombinant viruses were capable of replication and infectious virus production. The replacement of JFH-1 NS5A with those of genotype 1 strains resulted in similar or slightly reduced virus production, whereas replacement with those of genotype 2 strains enhanced virus production as compared with JFH-1 wild-type. A single cycle virus production assay with a CD81-negative cell line revealed that the efficient virus production elicited by replacement with genotype 2 strains depended on enhanced viral assembly, and that substitutions in the C-terminus of NS5A were responsible for this phenotype. Pulse-chase assays revealed that these substitutions in the C-terminus of NS5A were possibly associated with accelerated cleavage kinetics at the NS5A–NS5B site. Using this cell culture system with NS5A-substituted recombinant viruses, the anti-viral effects of an NS5A inhibitor were then examined. A 300- to 1000-fold difference in susceptibility to the inhibitor was found between strains of genotypes 1 and 2. This system will facilitate not only a better understanding of strain-specific roles of NS5A in the HCV lifecycle, but also enable the evaluation of genotype and strain dependency of NS5A inhibitors.

1. Introduction

Approximately 3% of the world's population is persistently infected with hepatitis C virus (HCV) and at increased risk of fatal chronic liver diseases such as decompensated liver cirrhosis and hepatocellular carcinoma. HCV have significant diversity in their genome and are grouped into six major genotypes. Among these genotypes, genotypes 1 and 2 are distributed worldwide and are predominant in Japan. The genotype is an important viral factor to predict the outcome of interferon (IFN)-based therapy. Because the efficacy of current therapy with pegylated IFN and ribavirin is insufficient, there is great interest in the development of novel HCV-specific inhibitors. The development of an HCV cell culture system with strain JFH-1 has enabled the study of the viral lifecycle and research into anti-viral compounds [1]. However, the available strains used in the HCV cell culture system are still limited to JFH-1 (genotype 2a) and H77S (genotype 1a) [2]. Thus, JFH-1 based recombinant viruses harboring specific regions of other strains would be useful to assess the genotype or strain-specific sensitivity to novel anti-HCV compounds.

Although NS5A is an essential and involved in HCV RNA replication and virus assembly [3,4], it has been reported to be tolerable for trans-complementation in replication-defective mutants due to critical mutations in NS5A [5]. We hypothesized that the NS5A of strain JFH-1 could be replaced with those of other strains. In the present study, we developed a cell culture system with JFH-1 based intra- and inter-genotypic recombinant HCV harboring NS5A of strains H77 (genotype 1a) [6], Con1 (genotype 1b) [7], J6CF (genotype 2a) [8], and MA (genotype 2b) [9]. Through the use of these recombinant viruses, we evaluated the effects of NS5A replacement on the HCV lifecycle and susceptibility to the NS5A inhibitor BMS-790052.

* Corresponding author. Address: Department of Virology II, National Institute of Infectious Diseases, 1-23-1 Toyama, Shinjuku-ku, Tokyo 162-8640, Japan. Fax: +81 3 5285 1161.
E-mail address: takato@nih.go.jp (T. Kato).

0006-291X/$ - see front matter © 2011 Elsevier Inc. All rights reserved.
doi:10.1016/j.bbrc.2011.05.144

2. Materials and methods

2.1. Cell culture

The human hepatoma cell line, HuH-7, and derivative cell lines, Huh7.5.1 [10] and Huh7-25 [11], were cultured in complete growth medium as described previously [1,11].

2.2. Plasmid construction

Plasmids containing the full-genome of HCV strain JFH-1 (pJFH1) and of a replication defective mutant (pJFH1/GND) have been described previously [1]. The construction of the NS5A replaced recombinant viruses and subgenomic reporter replicons was described in Supplementary materials.

2.3. In vitro RNA synthesis and RNA transfection

In vitro synthesis of HCV RNA and RNA transfection were performed as described elsewhere [1].

2.4. Quantification of HCV core protein, luciferase activity, and extra- and intra-cellular infectivity

Quantification of these values was described in Supplementary materials.

2.5. Inhibition of HCV production by a specific NS5A inhibitor

Huh7.5.1 cells (3×10^6) were electroporated with 3 μg of synthetic HCV RNA, suspended in 15 mL complete growth medium, and seeded into 24-well plates. At 4 h after electroporation, the culture medium was replaced with medium containing 0.1% dimethyl sulfoxide (DMSO) with or without various concentrations of the specific NS5A inhibitor BMS-790052 (provided from Bristol-Myers Squibb Company, Plainsboro, NJ) [12]. After 44 h incubation, cells were harvested and HCV core protein was quantified.

2.6. Statistical analysis

Unpaired 2-tailed *t*-test was performed to evaluate the significance of results, and $p < 0.05$ was considered significant.

3. Results

3.1. Development of recombinant HCV with NS5A of genotypes 1 and 2

To establish an HCV cell culture system with NS5A of various strains, we generated recombinant viruses by replacing NS5A of strain JFH-1 with those of genotypes 1 and 2 strains. By transfection of *in vitro* transcribed RNA, efficient production of HCV core protein was detected in JFH-1 wild-type (JFH1/wt) and other recombinant viruses, but not in the replication defective mutant JFH1/GND (Fig. 1A). When compared between JFH1/wt and other recombinant viruses, intracellular core protein levels were comparable at days 2 and 3 after transfection, while extracellular core protein levels were very different. The extracellular core protein level of JFH1/wt-transfected cells increased exponentially up to 23,515 ± 1790 fmol/L at day 3. Similar kinetics was observed in JFH1/5A-H77-transfected cells. However, the extracellular core protein level of JFH1/5A-Con1-transfected cells was approximately 2.5-fold lower than that of JFH1/wt at days 2 and 3. Interestingly, the extracellular core protein levels of intra-genotypic recombinant viruses, JFH1/5A-J6CF and 5A-MA, were 2.5- to 3.5-fold higher than that of JFH1/wt at days 2 and 3. To evaluate the effect of these NS5A replacements on HCV replication, we used recombinant subgenomic reporter replicons, SGR-JFH1/RLuc/wt, 5A-H77, 5A-Con1, 5A-J6CF, and 5A-MA. The *Renilla* luciferase activities of these recombinant subgenomic replicons were comparable to that of SGR-JFH1/Rluc/wt, suggesting similar levels of replication efficiency (Fig. 1B).

To further assess whether NS5A replacement affected other steps of the viral lifecycle, we used a single cycle virus production assay with Huh7-25 cells, a HuH-7-derived cell line lacking CD81 expression on the cell surface [11]. This cell line can support replication and infectious virus production upon transfection of HCV genomic RNA, but cannot be reinfected by produced HCV, therefore allowing the observation of a single cycle of infectious viral production without the confounding effects of reinfection [13]. As shown in Fig. 1C, JFH1/wt yielded an extracellular infectivity titer of 1585 ± 436 FFU/well at day 2 after transfection. JFH1/5A-H77 and 5A-Con1 showed significantly lower titers, while JFH1/5A-J6CF and 5A-MA showed significantly higher intracellular infectivity titers compared to JFH1/wt ($p < 0.05$). These data were consistent with the extracellular core protein levels of JFH1/wt and recombinant viruses (Fig. 1A). A similar tendency was observed in the intracellular infectivity titers of JFH1/wt and recombinant viruses (Fig. 1C). To estimate the efficiency of viral particle assembly, we determined the intracellular specific infectivity by calculating the ratio of the intracellular infectivity titer over the intracellular HCV core protein level. The intracellular specific infectivities of JFH1/5A-H77 and 5A-Con1 were 2.5- and 8-fold lower than that of JFH1/wt, respectively, while JFH1/5A-J6CF and 5A-MA showed 12- and 4-fold higher infectivities compared to JFH1/wt, respectively, suggesting a low assembly efficiency of JFH1/5A-H77 and 5A-Con1, and a high assembly efficiency of JFH1/5A-J6CF and 5A-MA (Fig. 1D). Taken together, all recombinant viruses could replicate and yielded infectious virus. Intra-genotypic recombinant viruses, JFH1/5A-J6CF and 5A-MA, had a higher ability to produce infectious virus than JFH1/wt in cultured cells.

3.2. The C-terminus of NS5A is responsible for enhanced viral assembly

The efficient infectious virus production of intra-genotypic recombinant viruses was unexpected. This prompted us to search for causes of the enhancement. To analyze the enhanced virus assembly of JFH1/5A-J6CF and 5A-MA, we focused on the C-terminus of NS5A of these strains, because this region influence the cleavage between NS5A and NS5B, and the cleavage is reported to be involved in virus assembly [14]. We generated recombinant JFH-1 viruses harboring 10 amino acids of the C-terminus of NS5A of J6CF and MA (JFH1/5AcJ6 and 5AcMA, respectively), and investigated replication and infectious virus production. In these 10 amino acids of the C-terminus of NS5A, JFH1/5AcJ6 and 5AcMA contain 2 and 6 substitutions, respectively, as compared with JFH1/wt, and 2 of them, T2438S and T2439V, are common (Fig. 2A). As shown in Fig. 2B, the extracellular core protein level of JFH1/5AcJ6-transfected cells was higher than those of JFH1/wt- and 5A-J6CF-transfected cells at the examined time points. A similar tendency was observed between JFH1/5AcMA and JFH1/wt or 5A-MA (Fig. 2C). In contrast to the extracellular core protein levels, the intracellular core protein levels were comparable for all NS5A recombinants at the examined time points.

We next assessed the replication of recombinant subgenomic luciferase reporter replicons on the basis of JFH1/5AcJ6 and 5AcMA (Fig. 2D). JFH1/5AcJ6 and 5AcMA showed similar levels of replication to JFH1/wt at day 2 after transfection. To investigate the effects of substitutions at the C-terminus of NS5A on infectious viral particle assembly, we determined the extra- and intracellular infectivity with the single cycle virus production assay with Huh7-25 cells. As shown in Fig. 2E, extra- and intracellular infectivities of